AD-A144 560 OPTIMAL SENSOR/ACTUATOR PLACEMENT ON A LARGE SPACE STRUCTURE(U) AIR FORCE INST OF TECH WRIGHT-PATTERSON AFB OH SCHOOL OF ENGINEERING R R LUTER MAR 84 1/1

UNCLASSIFIED AFIT/GA/AA/82D-6 F/G 22/1 NL

END

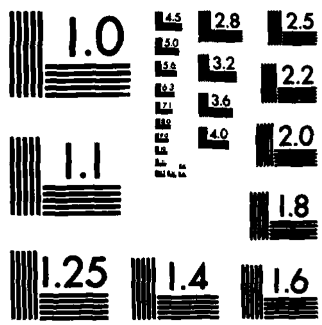

MICROCOPY RESOLUTION TEST CHART
NATIONAL BUREAU OF STANDARDS-1963-A

AD-A144 560

DTIC FILE COPY

OPTIMAL SENSOR/ACTUATOR
PLACEMENT ON A LARGE
SPACE STRUCTURE

THESIS

AFIT/GA/AA/82D-6 Robert R. Luter
1st Lt USAF

UNITED STATES AIR FORCE
AIR UNIVERSITY
AIR FORCE INSTITUTE OF TECHNOLOGY
Wright-Patterson Air Force Base, Ohio

84 08 20 093

AFIT/GA/AA/82D-6

OPTIMAL SENSOR/ACTUATOR PLACEMENT ON A LARGE SPACE STRUCTURE

THESIS

AFIT/GA/AA/82D-6 Robert R. Luter
1st Lt USAF

This document has been approved for public release and sale; its distribution is unlimited.

AFIT/GA/AA/82D-6

OPTIMAL SENSOR/ACTUATOR PLACEMENT ON A LARGE SPACE STRUCTURE

THESIS

Presented to the Faculty of the School of Engineering
of the Air Force Institute of Technology
Air University
in Partial Fulfillment of the
Requirements for the Degree of
Master of Science

by

Robert R. Luter, Jr., B. S.
1st Lt USAF

Graduate Astronautical Engineering

March 1984

A-1
DTIC COPY INSPECTED 2

Approved for public release; distribution unlimited

PREFACE

I would like to thank my thesis advisors, Major M. Wallace and Dr. R. Calico. Without their help and guidance the completion of this thesis would not have been possible.

Robert R. Luter, Jr.

Contents

List of Figures

List of Tables

List of Symbols

Symbol		
A	=	Plant Coefficient Matrix
B	=	Control System Matrix
$\vec{B} \cdot \vec{B}$	=	Dot Product
$\|\vec{B}\|$	=	$(\vec{B} \cdot \vec{B})^{1/2}$ - Norm or Magnitude
B^2	=	$(\vec{B} \cdot \vec{B})$ - Norm Squared
B_x	=	New Element of $\vec{B}$
C	=	Output System Matrix
C_p	=	Direction Cosine Matrix
D	=	Direction Cosine Matrix
E	=	Damping Matrix
$\vec{g}$	=	Generalized Coordinates
G	=	Control Feedback Gain Matrix
K	=	Stiffness Matrix, or Observer Gain Matrix
M	=	Mass Matrix
n_a	=	Number of Actuators
n_c	=	Number of Controlled Eigenvectors
n_s	=	Number of Sensors
$\vec{Q}$	=	Input Forces
$\vec{u}$	=	Actuator Force Inputs
$\vec{x}$	=	State Vector
$\vec{y}$	=	Output Vector
α	=	Angle Between Vector and Positive x Axis
β	=	Angle Between Vector and Positive y Axis
γ	=	Angle Between Vector and Positive z Axis

ζ = Damping Ratio

η = Modal Coordinates

ϕ = Modal Matrix

ω = Natural Frequency

ABSTRACT

The method of eliminating observation and control spillover by making groups of reduced order controlled modes orthogonal to each other is investigated. The orthogonality of these groups of modes is manipulated by changing the sensor/actuator model used on the structure. A sensor/actuator with variable location and orientation is added to the original model to implement a search for a systematic method of forcing modes into groups.

Perturbations in the structural model are also observed to see how model deficiencies affect the stability of coupling between modes. Mass changes did not affect the coupling significantly. NASTRAN is used to determine the eigenvectors, which are needed to make the orthogonality calculations.

The program ANGLE is developed to calculate the angles between the modes, given a sensor/actuator model and the critical modes taken from NASTRAN. Groups of modes for the decentralized controllers are identified and studied for possible improvements that can be achieved using sensor/actuator model changes.

After identifying likely improvable angles, the program ORIENT searches for sensor/actuator models that will indeed improve the desired angles. The ability to change one angle without significantly changing any others was found to be very difficult. The best method for improving the coupling characteristics is an iteration procedure: improve one angle at a time, then identify the next best way to improve the groupings, and repeat.

I Introduction

The ability of a large space structure to function as desired is dependent on the ability to control the structure. The controllability of the structure, however, is hindered by the capability of computer control systems. A solution to the problem is to use reduced order controllers.

Reducing the number of modes that are controlled introduces another problem. The uncontrolled modes will contaminate sensor data. This contamination by the uncontrolled modes produces observation and control spillover. Janiszewski (Ref 1) shows that the suppression of observation spillover allows the controller to be stable. Spillover is eliminated by forcing the off-diagonal terms of the control matrix to equal zero. Spillover terms can also be forced to zero by making groups of modes orthogonal to each other. This method of elimination was proposed by Miller (Ref 2).

The modes of the system matrices can be made orthogonal by the selected placement of actuators and sensors. Both the orientation and location of the actuators and sensors effect the orthogonality of the modes. Model groupings are made of modes that are coupled to each other, but decoupled from the other groups of modes. Miller suggests that the coupling characteristics be determined by calculating the angle between the modes using a dot product formula. This approach gives a clear method of measuring the coupling between modes. Therefore, we have a method for determining the modal groupings by calculating the coupling characteristics due to the sensor/actuator location and orientation model.

This investigation studied the effect on the coupling of the modes by the changing of the sensor/actuator model. The model has two parameters that are changed: the orientation and the location of the sensor/actuator pair. The first method that changes the model is implemented by adding a new sensor/actuator pair. This method allows a new and better sensor/actuator model to be chosen by adding one sensor/actuator pair at a time to the model in a systematic manner. This new sensor/actuator can be located at any node of the structure. Once a location is chosen, the possible orientation angles can be studied. After choosing a particular orientation (that gives favorable results), this sensor/actuator becomes part of the old model, and a new sensor/actuator is then studied. The primary investigation is to choose a sensor/actuator model that will achieve an acceptable modal grouping.

The second method changes the sensor/actuator orientations of the original model. The determination of the new orientations require close observation of the system matrices. The objective of this investigation is to choose the orientations so that the existing modal grouping is improved.

The last area of investigation is the effect the structural modeling has on the coupling characteristics and modal groupings. The structure is modeled with finite elements. These elements represent the actual structure. Thus, a structural change requires a change in the finite element model of the structure.

Changing the structural model can vary the only other parameter used in this study: the eigenvectors. Since structural modeling is not precise, the eigenvectors do not accurately represent the structure. The question is how much effect does this

inaccuracy have on the control of the structure? The structural analysis program NASTRAN is used to calculate the eigenvectors using the given finite element model. By changing this finite element model, inaccuracies of the structural model can be tested for their effect on the coupling angles between modes. This is done by calculating the coupling angles, using the new eigenvectors provided by the changed finite element model.

Throughout this study, a system model was used with a given set of sensor/actuator pairs. Position sensors and force actuators are used. Thus, only translational degrees of freedom are considered throughout this work. The sensors and actuators are collocated so the modal coupling characteristics will be the same for both observation and control spillover terms.

II Model

The large space structure model used in this study is the Charles Stark Draper Laboratory Model II (CSDL-II), Revision 3. The structure contains three mirrors, a focal plane, and the support trusses for the mirrors. It also has an equipment section and two solar panels. The model is shown in Fig 1.

Finite Element Model

Cook (Ref 3) defines finite element analysis as a numerical procedure for solving a continuum mechanics problem. Structures are approximated by elements that are connected by nodes. The CSDL-II structure consists of beams that form support trusses. These beams are modeled by three-dimensional frame elements, which allow bending, and axial stiffness. All of the elements in this model are frame elements.

The elements in the model represent hollow graphite epoxy tubes. The wall thicknesses of the tubes range from 0.03cm to 0.067cm. The radius ranges from 3.6cm to 8.1cm. Each element is designed so that it is only strong enough to meet local buckling and member natural frequency constraints. The natural frequency of each element has to be greater than 10hz so that local vibrations will not interact with system vibrations. For those interested, the buckling and natural frequency constraints, and the sizes and section properties of each element are given by Henderson (Ref 4:3-6); however, these properties were not used in this investigation.

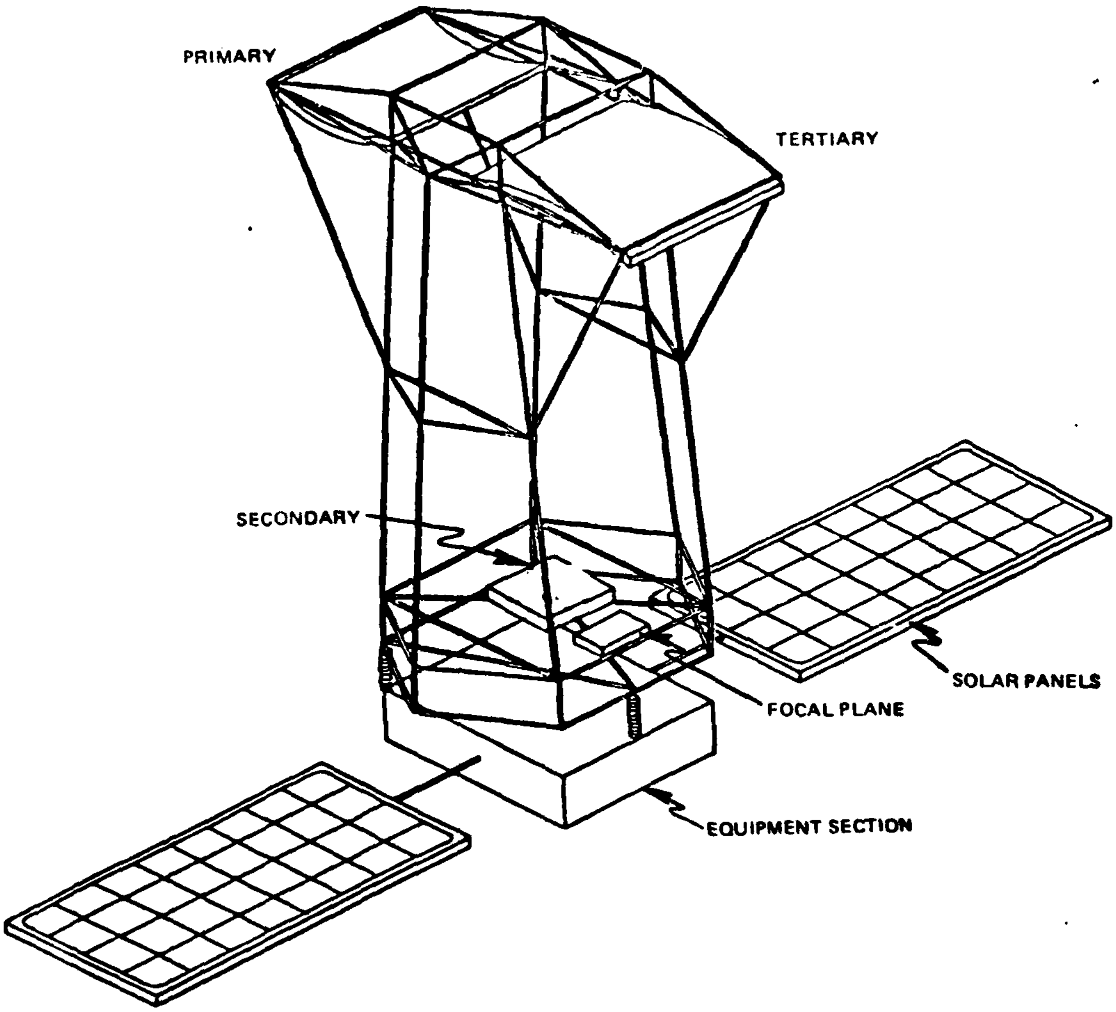

FIGURE 1 - CSDL Model II

Each element is connected to another by a single node. The structure has a total of 59 nodes with 23 lumped-mass nodes. These nodes, along with their masses, are cataloged in Table I. The locations of the nodes are shown in Fig 2.

The mass model is a revision of the previous model used for CSDL-II. In this revision, the mirror masses of the model are changed so that details of the support truss of the rigid mirrors can be modeled (Ref 4). The total mirror mass of the previous model is kept the same. However, the total mass of each mirror is now divided into two parts, the mirror mass and the optical support structure mass. Thus, nodes 1001, 1002, and 1003, the nodes at the center of each mirror, contain the lumped mirror masses. The nodes surrounding the mirrors have the lumped masses due to the optical support structure mass. Both the primary and tertiary mirrors already have a massive support truss at one end. Thus, this support mass has already been partially accounted for. Therefore, the mass of the support element is subtracted from the lumped optical support mass. This leads to large lumped masses (due to the optical support mass) at two corners and smaller masses (due to the optical mass minus the support truss mass) at the other two corners of each mirror, since that is where the massive support truss is located.

The finite element analysis is accomplished through the structural analysis program NASTRAN. Each element has stiffness properties, and some nodes have lumped-mass properties. Mass and stiffness matrices for the system are calculated by NASTRAN. These matrices allow NASTRAN to complete an eigenvector analysis. These eigenvectors are then used to calculate the coupling characteristics of the structure.

Table I

Node Location and Lumped Mass

NODE	X (M)	Y (M)	Z (M)	LUMPED MASS (KG)
1	-7.0	0.0	0.0	0.0
2	-4.0	5.0	0.0	0.0
3	-4.0	-5.0	0.0	0.0
4	0.0	5.0	0.0	0.0
5	4.0	5.0	0.0	0.0
6	4.0	-5.0	0.0	0.0
7	7.0	0.0	0.0	0.0
8	-7.0	0.0	2.0	0.0
9	-4.0	5.0	2.0	67.4
10	-4.0	-5.0	2.0	67.4
11	4.0	5.0	2.0	67.4
12	4.0	-5.0	2.0	67.4
13	7.0	0.0	2.0	0.0
14	-6.0	0.0	12.0	0.0
15	-4.0	4.0	12.0	0.0
16	-4.0	-4.0	12.0	0.0
17	4.0	4.0	12.0	0.0
18	4.0	-4.0	12.0	0.0
19	6.0	0.0	12.0	0.0
26	-5.0	0.0	22.0	0.0
27	-4.0	3.0	22.0	69.5
28	-4.0	-3.0	22.0	6.74
29	4.0	3.0	22.0	69.5

Table I

Node Location and Lumped Mass

(Continued)

NODE	X (M)	Y (M)	Z (M)	LUMPED MASS (KG)
30	4.0	-3.0	22.0	6.74
31	5.0	0.0	22.0	0.0
32	-4.0	10.0	22.0	6.74
33	4.0	10.0	22.0	6.74
34	-4.0	-10.0	22.0	69.5
35	4.0	-10.0	22.0	69.5
36	-4.0	3.0	24.0	0.0
37	-4.0	-3.0	24.0	0.0
38	4.0	3.0	24.0	0.0
39	4.0	-3.0	24.0	0.0
40	0.0	2.5	2.0	0.0
42	0.0	5.0	-0.3	0.0
43	-2.0	0.0	-1.3	0.0
44	0.0	-1.667	-1.3	3500.0
45	2.0	0.0	-1.3	0.0
46	-4.0	-5.0	-0.3	0.0
47	4.0	-5.0	-0.3	0.0
48	-26.0	0.0	-1.3	81.91
49	-21.0	0.0	-1.3	0.0
50	-16.0	0.0	-1.3	163.82
51	-11.0	0.0	-1.3	0.0
52	-6.0	0.0	-1.3	73.82
53	6.0	0.0	-1.3	73.82

Table I

Continued

NODE	X (M)	Y (M)	Z (M)	LUMPED MASS (KG)
54	11.0	0.0	-1.3	0.0
55	16.0	0.0	-1.3	163.82
56	21.0	0.0	-1.3	0.0
57	26.0	0.0	-1.3	81.91
100	0.0	0.0	0.0	0.0
910	-4.0	-2.5	2.0	0.0
1001	0.0	-6.5	22.0	1000.0
1002	0.0	0.0	2.0	800.0
1003	0.0	6.5	22.0	1200.0
1004	0.0	4.0	2.0	600.0
1112	4.0	-2.5	2.0	0.0
2830	0.0	-3.0	22.0	0.0
3233	0.0	10.0	22.0	0.0

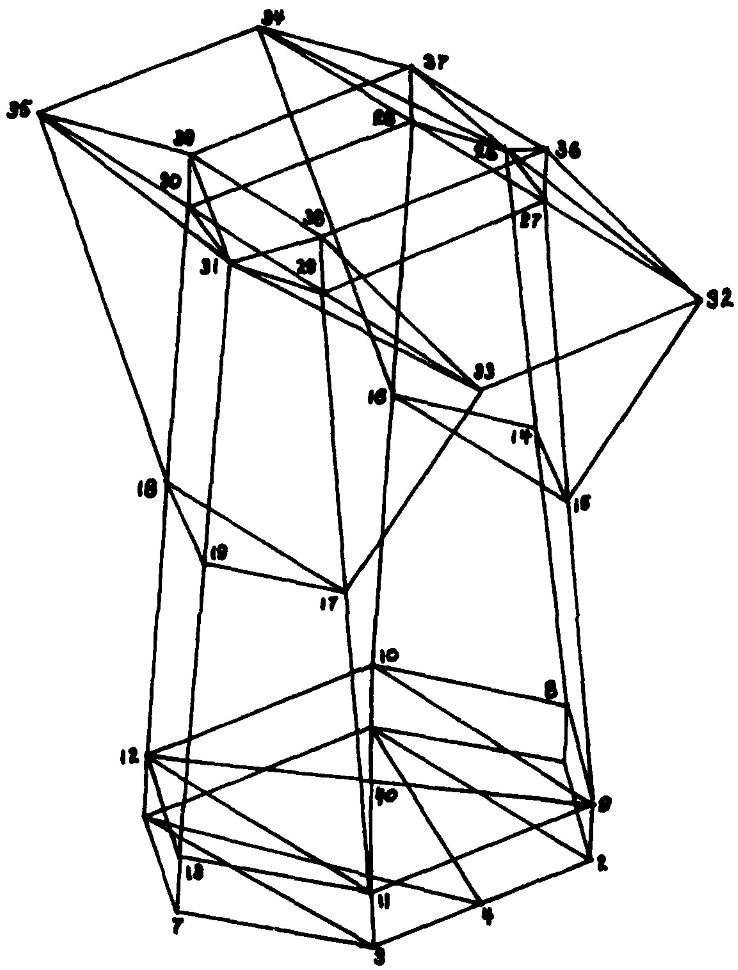

FIGURE 2 - Location of Nodes

The NASTRAN bulk data deck is listed in Appendix A. The bulk data deck produces a listing of the eigenvalues and eigenvectors for the finite element model. To change the modeling of the structure, the data deck is modified. New eigenvalues and eigenvectors will be produced with each change in the data deck.

The mass model of CSDL-II is modified by changing the lumped mass values in the data deck. This is accomplished through the CONM-2 statements. There is one CONM-2 line for each node that has a lumped mass (Appendix A). Each line contains the node number of the lumped mass and the value of the mass.

Sensor/Actuator Model

The sensor/actuator pairs' location and orientation are given in Table II. This model was suggested by CSDL (Ref 4). The suggestion is based on the line-of-sight (LOS) error. The LOS error is derived from the mathematical model given by CSDL (Ref 5). The error is a function of 21 coordinate variables. These 21 variables are the coordinates of 12 nodes that control the geometry of the optical path. Thus, to control the LOS error, these 21 coordinates were chosen for the sensor/actuator pairs locations.

Table II

Sensor/Actuator Nodes and Orientation

Number	NODE	ALPHA	BETA	GAMMA
1	9	90.00	0.00	90.00
2	9	90.00	90.00	0.00
3	10	90.00	90.00	0.00
4	11	0.00	90.00	90.00
5	11	90.00	0.00	90.00
6	11	90.00	90.00	0.00
7	12	90.00	90.00	0.00
8	27	0.00	90.00	90.00
9	27	90.00	0.00	90.00
10	27	90.00	90.00	0.00
11	28	90.00	90.00	0.00
12	29	90.00	0.00	90.00
13	29	90.00	90.00	0.00
14	30	90.00	90.00	0.00
15	32	90.00	90.00	0.00
16	33	90.00	90.00	0.00
17	34	0.00	90.00	90.00
18	34	90.00	0.00	90.00
19	34	90.00	90.00	0.00
20	35	90.00	0.00	90.00
21	35	90.00	90.00	0.00

Note that all of the sensor/actuator pairs are oriented along an axis direction as specified by the LOS equation. This restriction is not followed with sensor/actuator pairs that are added throughout the study.

III Theory

Equations of Motion

A vibrating structure has equations of motion

$$M \ddot{\vec{g}} + E \dot{\vec{g}} + K \vec{g} = \vec{Q} \qquad (1)$$

where $\vec{g}$ is a n-vector of generalized coordinates, M a n x n symmetric mass matrix, K a n x n symmetric stiffness matrix, E a n x n symmetric damping matrix, and $\vec{Q}$ a n-vector of input forces. This equation is also valid for large space structures such as the CSDL-II model.

The input force vector can be separated into two parts

$$\vec{Q} = D \vec{u} \qquad (2)$$

where D is a n x m matrix of direction cosines, and $\vec{u}$ is a m-vector of actuator force inputs. The direction cosine matrix, D, is block diagonal when there is only one actuator per node. The matrix columns contain the three direction cosines of the corresponding actuator force inputs. Equation 1 is simplified by using modal coordinates, η. Janiszewski shows that the equations can be expressed in state variable form

$$\dot{\vec{x}} = A \vec{x} + B \vec{u} \qquad (3)$$

where

$$\vec{x} = \{ \eta , \dot{\eta} \}^T$$

$$A = \left[\begin{array}{c|c} 0 & I \\ \hline -\omega^2 & -2\zeta\omega \end{array}\right]$$

$$B = \left[\begin{array}{c} 0 \\ \hline \phi^T D \end{array}\right]$$

the general output equation is

$$\vec{y} = C \vec{x} \qquad (4)$$

where

$$C = [\ C_p\phi,\ C_v\phi\ ]$$

The modal matrix, ϕ , is a matrix containing the eigenvectors of the structure by column. It is a matrix which is $n \times n_c$ where n is the number of degrees of freedom and n_c the number of controlled eigenvectors.

Since we only have point sensors and force actuators that are collocated, half of each matrix is filled with zeros. If the zero halves of these matrices are neglected, we may define

$$B^T = C \qquad (5)$$

or

$$D^T = C_p$$

where C_p is a $n_s \times n$ matrix of direction cosines corresponding to the sensors. The system matrices, B and C, are of order $n_c \times n_a$

and $n_s \times n_c$ respectively, where n_a is the number of actuators and n_s is the number of sensors.

Modal Coupling

In a complex structure where there are a large number of modes, a reduced order model is used. Janiszewski shows that only a subset of the total number of structural modes need to be controlled. If this subset of modes is still large, then multiple controllers are used.

Each controller is designed to operate on only a small number of the modeled modes, which are a subset of the structural modes. However, spillover terms occur because the controller actually operates on all the modes. Thus, these spillover terms need to be eliminated.

$$\begin{aligned} B_i\, G_j &= 0 \\ & \qquad i \neq j \qquad (6) \\ K_i\, C_j &= 0 \end{aligned}$$

where G is the control feedback gain matrix, and K is the observer gain matrix. The subscripts on the matrices correspond to groups of modes.

Miller shows that equations 6 are satisfied if the system matrices, B and C of each controller, can be made orthogonal to the remaining controllers. Therefore, the spillover terms are eliminated if groups of modes are found with the following property: All modes in a group are coupled, and each group is decoupled from the other groups.

The modes that have been referred to are actually the rows of B and the columns of C. Therefore, it is the rows of B (columns of C) that must be separated into modal groups. These rows (columns) are the eigenvectors multiplied by the direction cosine matrix.

The degree of coupling is measured by the angle between the modal vectors. For B, the angles between the rows are

$$\theta = \cos^{-1}\left[\frac{\vec{B}_i \cdot \vec{B}_j}{\|\vec{B}_i\| \quad \|\vec{B}_j\|}\right] \tag{7}$$

where $\vec{B}_i$ and $\vec{B}_j$ are rows i and j respectively of B and $\|\vec{B}_i\|$ is the norm of the i^{th} row vector of B. These angles can be made into a symmetric $n_c \times n_c$ matrix of angles.

For C, the angle is taken between the columns. With the collocation of sensors and actuators, the angle matrix produced from B and C are identical.

Location

The elements of B and C are functions of the location of the actuators and sensors. An element is determined from three values of an eigenvector from the modal matrix ϕ which are multiplied by the direction cosines of an actuator or sensor. Therefore, an element of B is

$$B_{ij} = \phi_{6 \cdot \text{node}(j)-5\; i} \cos\alpha_j + \phi_{6 \cdot \text{node}(j)-4\; i} \cos\beta_j + \phi_{6 \cdot \text{node}(j)-3\; i} \cos\gamma_j \tag{8a}$$

where node (j) is the node of the j'th actuator. If k = 6* node(j)-5, then the number, ϕ_{ki} is the k'th row element of the i'th eigenvector, ϕ_i in the modal matrix, ϕ. These matrices can also be determined as follows:

$$B = \left[\{\phi_1\} \; \{\phi_2\} \; --- \; \{\phi_{n_c}\} \right]^T [D]$$

$$= \begin{array}{c} \\ \\ \text{1ST} \\ \text{ACT.} \\ \\ \\ \\ \\ \text{3RD} \\ \text{ACT.} \\ \\ \\ \\ \\ \text{2ND} \\ \text{ACT.} \\ \\ \\ \\ \\ \\ \end{array} \begin{array}{c} \begin{array}{cccc} \phi_1 & \phi_2 & \phi_3 & \end{array} \\ \left[\begin{array}{cccc} \phi_{11} & \phi_{12} & \phi_{13} & --- \\ \phi_{21} & \phi_{22} & \phi_{23} & \\ \phi_{31} & \phi_{32} & \phi_{33} & \\ - & - & - & \\ - & - & - & \\ - & - & - & \\ \phi_{71} & \phi_{72} & \phi_{73} & \\ \phi_{81} & \phi_{82} & \phi_{83} & \\ \phi_{91} & \phi_{92} & \phi_{93} & \\ - & - & - & \\ - & - & - & \\ - & - & - & \\ \phi_{131} & \phi_{132} & \phi_{133} & \\ \phi_{141} & \phi_{142} & \phi_{143} & \\ \phi_{151} & \phi_{152} & \phi_{153} & \\ - & - & - & \\ - & - & - & \\ - & - & - & \\ \vdots & & & \end{array} \right]^T \end{array} \left[\begin{array}{cccc} c\alpha_1 & 0 & 0 & --- \\ c\beta_1 & 0 & 0 & \\ c\gamma_1 & 0 & 0 & \\ 0 & 0 & 0 & \\ 0 & 0 & 0 & \\ 0 & 0 & 0 & \\ 0 & 0 & c\alpha_3 & \\ 0 & 0 & c\beta_3 & \\ 0 & 0 & c\gamma_3 & \\ 0 & 0 & 0 & \\ 0 & 0 & 0 & \\ 0 & 0 & 0 & \\ 0 & c\alpha_2 & 0 & \\ 0 & c\beta_2 & 0 & \\ 0 & c\gamma_2 & 0 & \\ 0 & 0 & 0 & \\ 0 & 0 & 0 & \\ 0 & 0 & 0 & \\ \vdots & & & \end{array} \right] \qquad (8b)$$

where k = 1, 13, 7 for the first three actuators in this example. In this case, the three actuators are at nodes 1, 3, and 2, respectively. Thus, k for actuator 2 is calculated by 6x(3)-5.

Similarly, an element of C is given by

$$C_{ij} = \phi_{6 \cdot \text{node}(i)-5\ j} \cos\alpha_i + \phi_{6 \cdot \text{node}(i)-4\ j} \cos\beta_i + \phi_{6 \cdot \text{node}(i)-3\ j} \cos\gamma_i \qquad (9)$$

Note that by adding an actuator, a column is added to B. With a new sensor, a row is added to C. Also, if an extra eigenvector is added to the modal matrix ϕ, then a row is added to B and a column to C.

The magnitude of the elements of B and C is dependent on the magnitude of the eigenvectors with respect to the norm. If the eigenvectors have small values with respect to the norm at the location of the j'th actuator and i'th sensor, then the elements of B and C corresponding to the actuator and sensor will be small. So an element of the system matrices, B and C, can be made small if the actuator/sensor location is chosen so that the eigenvector value is small with respect to its norm. Likewise, if the value of the eigenvector is large with respect to its norm at a particular location, then the system matrix element will be large.

The angle between modes is dependent on the elements of the system matrices. Therefore, the angle is also a function of the location of the sensor/actuator pairs. Desired angles can be achieved by the judicious placement of sensor/actuator pairs. The addition of a sensor/actuator pair will allow the angles between modes to be varied, since a new and different element is added to each mode of the system matrices. Thus, the angle between modes is dependent on the system matrix which includes the new elements which are dependent on the new sensor actuator pair.

Adding an element to each mode of the system matrices will yield the following equation for the angles between two modes (using equation 7 with $\vec{A}$ and $\vec{B}$ the two modes):

$$\Theta = \cos^{-1}\left[\frac{A_1B_1 + A_2B_2 + \ldots + A_xB_x}{(A_1^2 + A_2^2 + \ldots + A_x^2)^{1/2}(B_1^2 + B_2^2 + \ldots + B_x^2)^{1/2}}\right] \qquad (10)$$

where A_x and B_x are the new elements of each mode.

This equation can be simplified

$$\Theta = \cos^{-1}\left[\frac{\vec{A}\cdot\vec{B} + A_xB_x}{(A^2+A_x^2)^{1/2}(B^2+B_x^2)^{1/2}}\right] \qquad (11)$$

where $A^2 = \sum_{i=1}^{n} A_i^2 \qquad B^2 = \sum_{i=1}^{n} B_i^2$

the dot product, $\vec{A} \cdot \vec{B}$ is taken without the new elements.

Equation (11) can be reduced if one of the new elements is equal to zero. Letting B_x equal zero, we have

$$\Theta = \cos^{-1}\left[\frac{\vec{A}\cdot\vec{B}}{(A^2+A_x^2)^{1/2}\ \|\vec{B}\|}\right] \qquad (12)$$

If A_x is also equal to zero, the angle does not change. However, the angle will change if A_x is not zero. No matter what value A_x is (the larger the better), the denominator of equation (12) must increase. Thus, this leads to the angle going to 90°. Therefore, to decouple two coupled modes, find a location where one mode has large (relative to norm) values and the other small values.

The change in the cosine of the angle can be determined by setting the previous cosine equal to the new cosine of the angle (equation 12).

$$\cos\theta = \left[\frac{\vec{A}\cdot\vec{B}}{\|\vec{A}\|\ \|\vec{B}\|}\right] = \left[\frac{\vec{A}\cdot\vec{B}}{(A^2+A_x^2)^{1/2}\ \|\vec{B}\|}\right]$$

Thus, the cosine of the angle will change by the factor

$$\frac{\|\vec{A}\|}{(A^2+A_x^2)^{1/2}} = \frac{(A^2)^{1/2}}{(A^2+A_x^2)^{1/2}}$$

$$= \frac{A}{(A^2+A_x^2)^{1/2}}$$

$$= \frac{1}{\left[1+\left(\frac{A_x}{A}\right)^2\right]^{1/2}} \qquad (13)$$

If A_x is small compared to the norm (taken without A_x), the cosine of the angle will not change.

A second case occurs if the new element product dominates the previous dot product. This case can occur when the original modes are decoupled, since the dot product is zero. The angle now reduces to

$$\theta = \cos^{-1}\left[\frac{A_x B_x}{(A^2+A_x^2)^{1/2}(B^2+B_x^2)^{1/2}}\right]$$

$$= \cos^{-1}\left[\frac{1}{\left[1+\left(\frac{A}{A_x}\right)^2\right]^{1/2}\left[1+\left(\frac{B}{B_x}\right)^2\right]^{1/2}}\right] \qquad (14)$$

The new angle approaches zero if the new elements are large compared to the previous norms. Thus, two modes can be coupled if a location for the sensor/actuator pair can be found, such that the new elements are large with regard to the norm. Therefore, one way of coupling two modes is to put a sensor/actuator pair at

a node where the eigenvector ϕ_i is large. Also, if the elements produced for the other modes are small, then only the modes for which the elements are large will have a significant change in their coupling characteristics.

There are two disadvantages to this method. First, even though the angles between two modes with two new small elements remain the same, the angle between modes with new small elements and modes with new large elements drastically change (they decouple as shown in equation (12)). Secondly, there is no guarantee that a node location and orientation will be found that will satisfy these angle conditions. This is because the location and orientation simply determine which values within the eigenvector are used. If the eigenvectors do not contain precisely the right values, it is impossible to pick a location and orientation.

Orientation

The location of the sensor/actuator pair determines which elements (determined by k) of the eigenvector are used in the element equation (8). The three elements chosen by the node location of the sensor/actuator are taken from each eigenvector and multiplied to the direction cosines of the sensor/actuator. After this calculation the elements of B then become only a function of the orientation (through matrix D). Thus, the set of orientation angles must be known so the element can be determined.

The orientation angles, α, β, and γ are related. If any two and the octant of the sensor/actuator are known, then the third can be determined. If α and β are known, γ is then determined as shown in Fig 3.

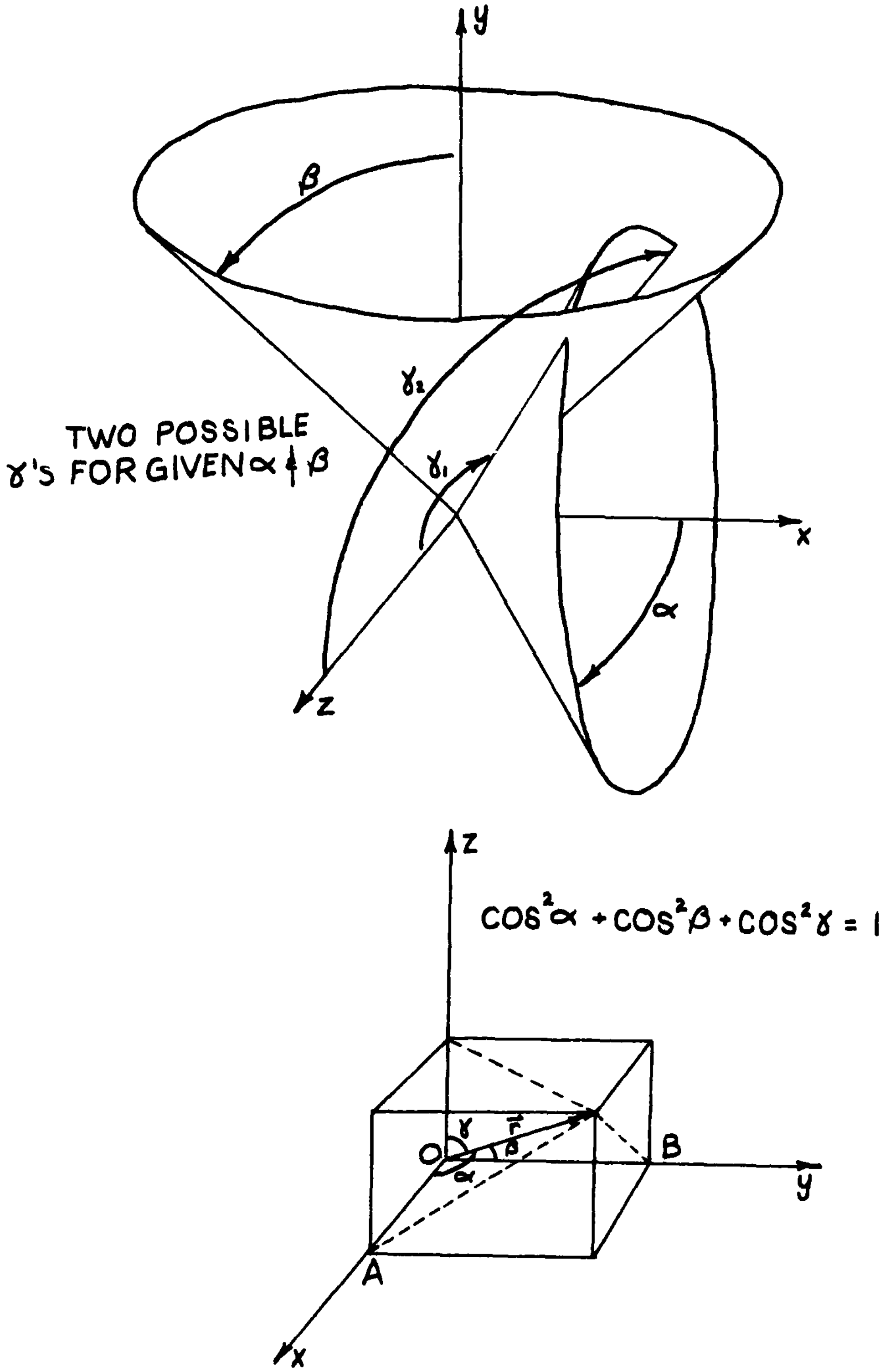

FIGURE 3 - Orientation Angles

$$\cos\alpha = \overrightarrow{OA}/\vec{r} = x$$
$$\cos\beta = \overrightarrow{OB}/\vec{r} = y \qquad (15)$$
$$\cos\gamma = \overrightarrow{OC}/\vec{r} = z$$

Since $\vec{r}$ is a unit vector, the direction cosines are equal to the components of the vector along the axes.

The magnitude of $\vec{r}$ is:

$$\|\vec{r}\| = \sqrt{x^2 + y^2 + z^2} = 1 \qquad (16)$$

Substituting equations (15) into equation (16)

$$\cos^2\alpha + \cos^2\beta + \cos^2\gamma = 1 \qquad (17)$$

Solving for γ , we have

$$\gamma = \cos^{-1}\sqrt{1 - [\cos^2\alpha + \cos^2\beta]} \qquad (18)$$

where α and β are varied from 0° to 180°.

All possible orientation angles can be tried, or specific orientations can be selected, so that existing elements of the B and C matrices are changed. The challenge in this procedure is to decide what the elements of these matrices should become in order for the modal angles to be acceptable. Then specific orientations are chosen so that the desired elements of the system matrices are produced.

Decoupled modes have a dot product equal to zero (relative to their norms). Thus, every large element of one mode will have a corresponding term in the other mode that is small (relative to norms). This correspondence between the modes causes the dot product to go to zero, which leads to decoupled modes. Another possibility is that large products have negative products that cancel them.

Coupled modes have the opposite condition: large elements correspond to each other, and small elements correspond to each other. Thus, the dot product equals the product of the norms.

By changing the sensor/actuator orientation, these conditions can be switched. The mode elements for the decoupled modes need to cause the dot product to increase in magnitude or the norms to decrease. This is accomplished by causing an element pair (one corresponding large and small element) to become both small or both large.

The coupled modes are decoupled by decreasing the dot product or increasing the norms. Again, this is accomplished by causing an element pair, that has either both large or both small elements to readjust, so that the element pair has one large element and one small element. Note again, all magnitudes above are relative to the norms.

Modes

Twelve eigenvectors were suggested by LMSC (Ref 6) to be the critical modes. These modes are listed in Table III. The modes were selected according to three criteria: modal cost, controllability, and observability. Ten modes were selected that had the highest controllability/observability product. Also, two modes were selected with the highest modal cost. These modes were used throughout this study as the critical modes.

These modes can change when the eigenvectors themselves change. With each perturbation of the finite element model, the eigenvectors (ϕ matrix) may change. This change obviously changes the modes (B and C matrices). This was the only change to the modes that was studied.

Table III

Mode-Eigenvector Correspondence

Mode	Eigenvector
1	4
2	5
3	6
4	7
5	12
6	13
7	17
8	21
9	22
10	24
11	28
12	30

Computer Programs

The computer programs used in this study are: NASTRAN, SELECT, ANGLE, and two versions of ORIENT. As stated previously, NASTRAN is used to perform a finite element analysis of CSDL-II. The program outputs the eigenvectors and eigenvalues into a permanent file. This file of eigenvectors is the basis for the other programs.

SELECT is listed in Appendix B. The purpose of this program is to pick off the eigenvectors output by NASTRAN. Any combination of eigenvectors in any order can be selected. The eigenvectors' numbers are first read by the program. The file of eigenvectors is stored in a three-dimensional matrix. Then, the selected eigenvectors are put into an output permanent file.

ANGLE is listed in Appendix C. ANGLE inputs the modal vector (from SELECT), and a sensor/actuator model that has been chosen. It then calculates the B, C, and angle matrices. The B and C matrices are calculated from the element equations (8-9). The angle matrix is determined by using the cosine equation (7). The angle matrix is then used to determine modal groupings.

ORIENT is the program that determines the orientation for each node location that will meet the desired requirements. Two diverse versions of ORIENT are used to determine the acceptable orientations. Both work by eliminating those orientations that do not meet the criteria (below). Version two is listed in Appendix D.

The first version of ORIENT tries to find the orientations that will cause large (relative to the norms) elemental values in two modes, but small elemental values in all other modes. It does this by checking the values of each new element. If the two modes in question were previously coupled, they would then be decoupled.

The second version simply prints all orientations that have the modes in a given set of modal groupings. The criteria used, if the modes are to be coupled, is that the angle must be less than 82° or greater than 103°. If the modes are to be decoupled, then the angle must be between 86° and 97°. Obviously it is desired to have coupled angles at 0° or 180°, and decoupled angles at 90°, but it is not possible to move all the modal angles to these desired angles. These specific angles were chosen so that already acceptable modal angles would fall within their limits and not have to change. Yet the worst angles would have to change. Note that this program is very versatile because conditions can be changed so that almost any objective can be investigated. If the modal groupings need to be changed, all that has to be changed is the input mode numbers. Similarly, the bounds for coupling and decoupling can be easily changed.

IV Investigation

Sensor/Actuator Model

The thrust of the investigation is to observe the coupling characteristics of the B and C matrices due to changes in the sensor/actuator model. Thus, determining matrices B and C is the first objective. Using the given sensor/actuator model, the matrices are calculated.

These matrices are found through the ANGLE program. The program was run originally with 17 modes; however, five eigenvectors were dropped: 11, 14, 16, 26, 29 (modes 13, 14, 15, 16, 17). This was done to simplify the problem (fewer modal angles). The five modes dropped had the lowest modal cost and controllability/observability product of the 17 eigenvectors. Thus, the 12 modes left were used as critical modes throughout the rest of the investigation.

Next, the angle between the modes was calculated using ANGLE. The results are in the form of a symmetric matrix where the rows and columns correspond to the mode numbers. Therefore, a 12 x 12 angle matrix is determined (see Table IV).

The purpose of calculating the angles between the modes is to determine modal groupings. These groupings are then used by the different controllers. The original sensor/actuator model produced three groups of modes that are in general orthogonal to each other or coupled within; however, the angles do not necessarily do both. Since modes 11 and 12 are decoupled, a second modal grouping is also possible. These two possible groupings are shown in Table V.

Both groupings have problems. The problem angles of the first group are circled in Table IV, while the second group's problem angles are boxed. These angles are a problem because they are not as nicely coupled or decoupled as the other angles. The first grouping has decoupled modes 11 and 12 in group II, where they should be coupled. The angles between modes 2-5, 2-9, 4-5, 4-9, and 8-10 indicate coupling, but these modes are in different groups (so, should be decoupled). The second grouping puts mode 12 into group III. While this separates modes 11 and 12, mode 12 is still coupled to modes 1, 6 and 7 in group II.

Table IV

Angle Matrix with Original Sensor/Actuator Model

	1	2	3	4	5	6
1	0.0000	89.9876	89.9991	90.9987	90.0884	123.2047
2	89.9876	0.0000	67.4653	175.3876	116.8521	90.0533
3	89.9991	67.4653	0.0000	115.3141	104.0098	89.9855
4	90.0087	175.3876	115.3141	0.000	60.6688	89.9526
5	90.0884	116.8521	104.0098	60.6688	0.0000	89.6936
6	123.2047	90.0533	89.9855	89.9526	89.6936	0.0000
7	107.4792	89.9662	90.0376	90.0220	90.0156	61.2182
8	90.0478	106.5687	116.9917	73.1913	102.7661	90.0720
9	90.0128	116.2323	91.5675	66.4898	68.5695	89.8722
10	90.0066	90.1561	80.1261	90.6814	111.8732	90.1536
11	39.1619	87.8879	89.4097	92.4490	96.6087	104.9007
12	$\boxed{81.1169}$	87.9411	89.2693	92.3517	95.6278	$\boxed{73.2904}$

	7	8	9	10	11	12
1	107.4792	90.0478	90.0128	90.0066	39.1649	$\boxed{81.1169}$
2	89.9662	106.5687	116.2323	90.1561	87.8879	87.9411
3	90.0376	116.9917	91.5675	80.1261	89.4097	89.2693
4	90.0220	73.1913	66.4898	90.6814	92.4490	92.3517
5	90.0156	102.7661	68.5695	111.8732	96.6087	95.6278
6	61.2182	90.0720	89.8722	90.1536	104.9007	$\boxed{73.2804}$
7	0.0000	89.9103	90.1494	89.9571	80.5616	$\boxed{127.8041}$
8	89.9103	0.0000	93.8830	38.0463	93.4985	93.1822
9	90.1494	93.8830	0.0000	103.2217	90.5112	90.7436
10	89.9571	38.0463	103.2217	0.0000	94.1486	93.4051
11	80.5613	93.4985	90.5118	94.1486	0.0000	89.8169
12	$\boxed{127.8041}$	93.1022	90.7436	93.4951	89.8169	0.0000

Table V

Modal Groupings

	I	II	III
CASE I	2	1	5
	3	6	9
	4	7	10
	8	11	
		12	
CASE II	2	1	5
	3	6	9
	4	7	10
	8	11	12

The two groupings represent two approaches to the problem of modes 11 and 12. The first grouping is an attempt to couple the two modes together. The second grouping places mode 12 into group III. This grouping tries to decouple mode 12 from the other modes in group II. This first approach is the simpler of the two. It is easier to couple modes together, since all that is needed is a change of about 10° off 90°. Although this is not much of a change, it is probably good enough for the controller to work.

To couple the modes together, the sensor/actuator model is changed. The original model stayed constant, but a new sensor/actuator pair was added. This pair could be placed at any location and at any orientation. The decision on where to place the sensor/actuator and at what orientation is complicated. This complication arises because every location and orientation chosen will change every angle between the modes.

To combat this problem, the two versions of ORIENT pick out the orientations that will couple modes 11 and 12, but leave the others in the same modal groupings.

Both versions try every node point location. This is because there is no way of knowing which node point is the best. Attempts to rank the nodes were not precise enough to eliminate the other nodes from consideration. Therefore, it was better to look at every node than to discard any of the nodes.

After the program picks a node, ORIENT checks all possible orientations which will satisfy the coupling conditions. ORIENT checks the orientations by calculating the modal angles until one is rejected. If an angle is rejected, the next orientation is

tried; if all angles are accepted, the angle matrix is then printed. Most of the orientations are discarded, but the output still has many orientations that will satisfy minimum conditions. The output orientations from ORIENT were then checked by hand to determine the best orientation that gives acceptable groupings. The determination of the best orientation necessarily chooses the best node location.

The next consideration of sensor/actuator model changes is that of changing the grouping. The first grouping was chosen because it was an acceptable grouping of the original sensor/actuator model. This grouping and the second one described above are not the only acceptable groupings. It does not matter which modes are in a given group, as long as they are coupled to each other, and decoupled from all other modes. This leads to an investigation of what other modal groupings are possible with a sensor/actuator model change.

Again, modes 11 and 12 were considered. ORIENT was run with two cases. Case one is that modes 11 and 12 be decoupled. Case two is that modes 11 and 12 be coupled. No other restrictions are made. This gives an output of all possible modal grouping where 11 and 12 are either coupled or decoupled.

The last type of model change investigated was changing the original sensor/actuator orientations. This modal change was investigated to see if the original orientations are indeed the best. Two extremes were studied. First, change the orientation so that decoupled modes are coupled. Second, decouple the coupled modes. The hope was that only the angles of the modes in question would be radically changed. The modal angles (old), the coupling

objectives, and the new sensor/ actuator orientations are listed in Table VI. In each run of the ANGLE program, only one sensor/ actuator orientation was changed. Again, this was done to keep other angles from changing too much.

TABLE VI

Original Sensor/Actuator Model Orientation Changes

MODES	OLD ANGLE	OBJECT	ACTUATOR	ORIENTATION CHANGES ALPHA	BETA	GAMMA
11-12	89.8°	Couple	2	0°	90°	90°
11-12	89.8°	Couple	13	90°	45°	45°
11-12	89.8°	Couple	10	90°	45°	45°
8-10	38°	Decouple	5	45°	45°	90°
8-10	38°	Decouple	10	45°	90°	45°
8-10	38°	Decouple	12	90°	45°	45°
8-9	93.8°	Couple	21	45°	90°	45°
7-10	89.4°	Couple	4	45°	45°	90°
7-10	89.4°	Couple	3	90°	0°	90°

Mass Model Changes

Determining the sensor/actuator pairs' location and orientation that produce a good grouping of modes is only valid for the structural model that has those eigenvectors used in the determination. If the structural model is in error, then the eigenvectors are in error. This error in the eigenvectors may change the coupling angles between the modes. If the coupling characteristics are drastically changed, the modal grouping could be different. This change in the grouping is unacceptable.

This problem led to finite element model changes being studied. Five different model changes were made. These are shown in Table VII. The first three are error percentage changes in the total mass of the tertiary mirror. A percentage of the total mass is added in proportion to each node. The fourth model keeps the same total mass but changes the proportion of mass at each node. The fifth model adds mass to the nodes with smaller mass amounts. The mass amount added equalizes the mass at each corner node.

All five mass changes were on the tertiary mirror. This mirror was chosen so that the structural model could be tested without symmetry effects. Since only this mirror would receive mass changes, no symmetry sensitive eigenvectors would go unaffected by the changes. Also, the three different types of mass changes further decreased this possibility.

NASTRAN was then run with each of the new models. This produced new eigenvectors for each model. After picking off the critical eigenvectors, ANGLE was run to determine the coupling angles between the modes. The sensitivity of the modal groupings to the mass modeling changes made to the tertiary mirror was then observed.

TABLE VII

Mass (kg) Changes

NODE	ORIGINAL	2% ADDED	10% ADDED	20% ADDED	PROPORTION CHANGE	EQUAL CORNERS
27	69.5	70.89	76.45	83.40	121.70	69.5
29	69.5	70.89	76.45	83.40	121.70	69.5
32	6.74	6.87	7.414	8.088	13.52	69.5
33	6.74	6.87	7.414	8.088	13.52	69.5
1003	1200	1224	1320	1440	1082	1200

V Results

The results of this investigation come from two sources. First, the sensor/actuator model is manipulated with the objective of obtain an acceptable grouping of modes. Further, the model is changed again to improve the selected groupings. Also, changes of the original orientations are studied. Second, the finite element model is perturbed so mass modeling errors can be observed. Specifically, the lumped masses at the nodes are changed.

Sensor/Actuator Model

The original sensor/actuator model is listed in Table II. The ANGLE program was run using this data. The angles between the modes are given in Table IV. By observing these coupling angles, modal groupings were picked out. The two groupings chosen are listed in Table V.

The results of ORIENT runs are mixed. When requirements of acceptance (see Appendix D) were too strict, no sensor/actuator models were found. This predicament was caused by some modal coupling angles being too far off the desired angles. In other words, the angles were required to be so close to either coupled (0° or 180°) or decoupled (90°) that some bad angles could not move inside the limits. These are the problem angles listed in the investigation section. Thus, these particular problem angles were then excluded from the acceptance requirements of ORIENT. The only exception is the angle between modes 11 and 12. Since this angle was one of the worst, it was singled out to continue to try to meet the acceptance limits. The results from ORIENT with

these new requirements of acceptance (most problem angles excluded) give node 42 as the best location. There were fifteen orientation that were acceptable at this location. The orientation that appears to be the best is:

$$\alpha = 90. \quad \beta = 90. \quad \gamma = 0.$$

This angle matrix is listed in Table VIII. Note that modes 11 and 12 have completely coupled. Also, while angles 1-6 and 1-11 have become worse, in general, the coupling characteristics have improve. Specifically, observe the marked improvement between modes 6-11, 6-12, 7-11 and 7-12. The decoupling has also improved throughout. The above noted improved angles are circled; the worse angles are boxed.

The ORIENT run for the second grouping produced no orientations. More exclusions from the requirements for acceptance need to be made before orientations are found. The new sensor/actuator pair picked for the previous grouping is not acceptable for this grouping. This is seen from the fact that coupling between mode 12 and group II increases instead of decreasing.

The next objective in changing the sensor/actuator model was to create new groupings. When modes 11 and 12 were decoupled, they determined two of the three groups. When the modes were coupled, only one group was determined. Two of the possibilities for groupings that were found (one for 11 and 12 coupled, one for them decoupled) are shown in Table IX and Table X. The mode groups for the coupled case are:

I: 1, 6, 7

II: 2, 3, 4, 5

III: 8,9, 10, 11, 12

The mode groups for the decoupled case are:

I: 6, 7, 12

II: 1, 5, 10, 11

III: 2, 3, 4, 8, 9

The two cases studied should have produced most of the possible mode grouping combinations; however, no radical improvements were noted with any sensor/actuator model.

TABLE VIII

Angle Matrix with Modes 11 & 12 Coupled

	1	2	3	4	5	6
1	0.000	89.9870	89.9990	90.0098	90.0541	$\boxed{106.5464}$
2	89.9870	0.0000	67.4653	175.3876	116.8520	90.0434
3	89.9990	67.4653	0.0000	115.3141	104.0988	89.9875
4	90.0098	175.3876	115.3141	0.0000	60.6688	89.9621
5	90.0541	116.8520	104.0098	60.6688	0.0000	89.6876
6	$\boxed{106.5464}$	90.0434	89.9875	89.9621	89.6876	0.0000
7	79.1801	89.9845	90.0128	90.0123	89.9137	50.7986
8	90.0119	106.5687	116.9916	73.1913	102.7659	90.0044
9	90.0215	116.2323	91.5675	66.4898	68.5696	89.9067
10	89.9951	90.1561	80.1261	90.6814	111.8731	90.1120
11	$\boxed{107.6054}$	89.9918	89.9969	90.0092	90.1359	121.5170
12	107.7985	89.9893	89.9951	90.0118	90.1379	121.3143

	7	8	9	10	11	12
1	79.1801	90.0119	90.0215	89.9951	$\boxed{107.6054}$	107.7885
2	89.9845	106.5687	116.2323	90.1561	89.9918	89.9893
3	90.0128	116.9916	91.3675	80.1281	89.9969	89.9851
4	90.0123	73.1913	66.4898	90.6814	90.0092	90.8110
5	89.9137	102.7659	68.5696	111.8731	90.1359	90.1379
6	50.7986	90.0044	89.9067	90.1120	121.5170	121.3143
7	0.0000	89.8663	90.0804	89.9508	159.5259	159.8303
8	89.8663	0.0000	93.8831	38.0463	90.1295	80.1314
9	90.0804	93.8831	0.0000	103.2217	89.9727	89.7518
10	89.9508	38.0463	103.2217	0.0000	90.0604	90.0614
11	159.5259	90.1295	89.9727	90.0604	0.0000	0.5249
12	159.8303	80.1314	89.9751	90.0614	0.5245	0.0000

TABLE IX

Angle Matrix for New Grouping (11 & 12 Coupled)

	1	2	3	4	5	6
1	0.0000	91.3907	91.7781	88.1414	81.4930	123.5268
2	91.3907	0.0000	65.1063	173.7748	112.3636	88.8425
3	91.7789	65.1063	0.0000	118.3582	99.4407	88.4525
4	88.1414	173.7748	118.3582	0.0000	66.9967	91.5642
5	91.4930	112.3436	99.4407	66.9967	0.0000	88.4894
6	123.5268	88.8425	88.4525	91.5642	88.4894	0.0000
7	109.2235	87.8575	87.3593	92.8293	87.8982	60.7614
8	95.9688	83.5529	83.4629	100.4695	82.2686	84.8955
9	93.3296	104.5331	82.8228	80.2084	65.1712	87.0308
10	89.4517	91.2650	81.9931	89.1670	112.4157	90.6307
11	83.3505	102.7891	106.3187	72.8646	102.8915	95.5664
12	83.5714	102.7831	106.3152	72.8712	102.9008	95.3021

	7	8	9	10	11	12
1	108.2235	95.9688	93.3296	89.4517	[illegible].3505	83.5714
2	87.8575	83.5529	104.5331	91.2650	102.7891	102.7831
3	87.3593	83.4629	82.8228	81.9931	106.3187	106.3152
4	92.8263	100.4695	80.2084	89.1678	72.8646	72.9712
5	87.8982	82.2686	65.1712	112.4157	102.8915	102.9009
6	60.7614	84.8955	87.0308	90.6307	95.5664	95.3021
7	0.0000	80.9959	85.1309	90.7925	99.4980	99.3388
8	80.9959	0.0000	61.8256	79.1714	159.8746	159.8771
9	85.1309	61.8256	0.0000	103.8861	121.6093	121.6123
10	90.7925	79.1714	103.8861	0.0000	84.9988	85.0043
11	99.4980	159.8746	121.6093	84.9988	0.0000	0.6887
12	99.9088	159.8771	121.6123	85.0047	0.6887	0.0000

TABLE X

Angle Matrix for New Grouping (11 & 12 Decoupled)

	1	2	3	4	5	6
1	0.0000	90.8174	90.7932	88.9493	86.7474	122.0821
2	90.8174	0.0000	66.7463	174.9228	116.6676	86.3539
3	90.7932	66.7483	0.0000	116.1557	105.8840	86.4521
4	88.9493	174.9228	116.1557	0.0000	60.1485	94.6762
5	86.7474	116.6676	105.8840	60.0485	0.0000	104.7235
6	122.0821	86.3539	86.4521	94.6762	104.7235	0.0000
7	108.3965	87.8155	87.9756	92.7696	98.6674	57.6279
8	90.3337	105.9797	116.2828	74.0025	102.1147	88.7901
9	89.8009	116.2560	91.8262	66.5076	71.1859	90.8291
10	90.4521	89.5529	79.6591	91.4364	110.4766	88.1533
11	39.4739	87.9660	89.4698	92.3365	95.2409	103.3852
12	82.9303	86.0350	87.3952	94.7842	102.5730	68.8043

	7	8	9	10	11	12
1	108.3965	90.3337	89.8009	90.4521	39.4739	82.8303
2	87.8155	105.9797	116.2560	89.5529	87.9660	86.0350
3	87.9759	116.2828	91.8262	79.6591	89.4698	87.3952
4	92.7696	74.0028	66.5076	91.4364	92.3365	94.7842
5	98.6674	102.1147	71.1859	110.4766	95.2409	102.5780
6	57.6279	88.7901	90.8291	88.1533	103.3852	68.8043
7	0.0000	89.1711	90.6934	88.8029	81.0230	120.3491
8	89.1711	0.0000	93.9749	38.0012	93.5142	92.3150
9	90.6934	93.9749	0.0000	103.3329	90.4969	91.2274
10	88.8029	38.0012	103.3329	0.0000	94.1676	92.3073
11	81.0230	83.5142	90.4969	94.1676	0.0000	89.9243
12	120.3791	92.3150	91.2274	92.3073	89.9243	0.0000

The results produced by changing the original model orientations are listed in Table XI. The table lists the new angles produced and the delta change from the old angles. The plus and minus signs indicate favorable or unfavorable changes respectively (i.e., minus sign if new angle is now more coupled, but the desire was to be more decoupled). The results show six of nine favorable changes overall; however, there are five of six favorable changes when the desire was to couple (first three and last three). It seems to be easier (I don't know why) to couple the angles than to decouple the angles.

The magnitude of the changes are small especially for the three cases where decoupling was the object. Yet, the largest changes (8.5° and 8.1°) are significant angle movements when it is remembered that only one sensor/actuator orientation was changed for each case. Note that when the angle changes are unfavorable, the magnitude of the changes are small (0.3 is the largest).

TABLE XI

Results From Original Orientations Changes

MODES	ACTUATOR	ORIENTATION CHANGES ALPHA	BETA	GAMMA	NEW ANGLE	DELTA CHANGE
11-12	2	0°	90°	90°	81.7°	$+8.1^{\circ}$
11-12	13	90°	45°	45°	91.8°	$+1.6^{\circ}$
11-12	10	90°	45°	45°	92.6°	$+2.4^{\circ}$
8-10	5	45°	45°	90°	37.9°	-0.1°
8-10	10	45°	90°	45°	38.3°	$+0.3^{\circ}$
8-10	12	90°	45°	45°	37.7°	-0.3°
8-9	21	45°	90°	45°	99.3°	$+5.5^{\circ}$
7-10	4	45°	45°	90°	89.6°	-0.2°
7-10	3	90°	0°	90°	99.1°	$+8.5^{\circ}$

Mass Model

The angle matrices produced from the mass model changes are cataloged in Table XII through Table XVI. Note that while some changes in angles did occur, the original groupings stayed the same. This can be seen by comparing Tables IV with these new tables.

The greatest angle changes were found in Table XVI (angles are circled). A 10° change occurred between modes 9-10. Modes 2-10 and 4-10 had 6° changes. All other angles in the model changes had angle changes of less than 3°. These results indicate that mode 10 is more sensitive than the other modes to the tertiary mirror mass model changes that caused Table XVI. That model change was the one with equal masses at the corners of the tertiary mirror. However, in general, the structural model is insensitive with respect to modal angles to the tertiary mirror lumped mass model changes tried.

TABLE XII

Angle Matrix with 2% Mass Change

	1	2	3	4	5	6
1	0.0000	89.9877	89.9990	90.0086	90.0890	56.7100
2	89.9877	0.0000	67.2166	175.3286	116.8176	89.9474
3	89.9990	67.2166	0.0000	115.6233	104.0412	90.0152
4	90.0086	175.3289	115.6233	0.0000	60.6811	90.0465
5	90.0880	116.8176	104.0412	60.6811	0.0000	90.3062
6	55.7100	89.9474	90.0142	90.0465	90.3062	0.0000
7	72.4413	90.0340	89.9624	89.9781	89.9860	61.0909
8	90.0469	106.7655	116.8679	73.0010	102.7656	89.9273
9	90.0131	116.3286	91.6029	66.4258	68.6255	90.1274
10	90.0053	90.0124	80.1219	90.8335	112.0084	89.8454
11	39.3911	87.8653	89.4109	92.4748	96.6414	75.1253
12	81.3855	87.9198	89.2806	92.3748	95.6397	107.0160

	7	8	9	10	11	12
1	72.4413	90.0469	90.0131	90.0053	39.3911	81.3855
2	90.0340	106.7655	116.3296	90.0124	87.8653	87.9198
3	89.9624	116.8679	91.6029	80.1219	89.4109	89.2806
4	89.9781	73.0010	66.4258	90.8335	92.4749	92.3748
5	89.9860	102.7656	68.6255	112.0084	96.6414	95.6397
6	61.0909	89.9273	90.1274	89.8454	75.1253	107.0160
7	0.0000	90.0882	89.8507	90.0423	99.278	52.6260
8	90.0882	0.0000	93.6552	38.0181	93.5231	93.1494
9	89.8507	93.6552	0.0000	103.4248	90.5090	90.7426
10	90.0423	38.0181	103.4248	0.0000	94.1647	93.5417
11	99.5278	93.5231	90.5090	94.1647	0.0000	89.9618
12	52.6260	93.1494	90.7426	93.5417	89.9618	0.0000

TABLE XIII

Angle Matrix with 10% Mass Change

	1	2	3	4	5	6
1	0.0000	89.9880	89.9989	90.0081	90.0912	123.6228
2	89.9880	0.0000	66.2873	175.1010	116.7026	90.0511
3	89.9989	66.2873	0.0000	116.7874	104.1296	89.9839
4	90.0081	175.1010	116.7874	0.0000	60.7141	89.9552
5	90.0912	116.7026	104.1296	60.7141	0.0000	89.6929
6	123.6228	90.0511	89.9839	89.9552	89.6929	0.0000
7	72.1172	90.0348	89.9626	89.9777	89.9922	119.4366
8	90.0438	107.4692	116.4368	72.3223	102.7904	90.0741
9	90.0143	116.6894	91.7448	66.1947	68.8212	89.8733
10	90.0006	89.5301	80.1183	91.3542	112.4773	90.1582
11	40.2559	87.7743	89.4148	92.5773	96.7645	104.7872
12	82.4133	87.8332	89.2694	92.4708	95.7364	71.8194

	7	8	9	10	11	12
1	72.1172	90.0438	90.0143	90.0006	40.2559	82.4133
2	90.0348	107.4692	116.6894	89.5301	87.7743	87.8332
3	89.9626	116.4368	91.7448	80.1183	89.4148	89.2694
4	89.9777	72.3223	66.1947	91.3542	92.5773	92.4708
5	89.9922	102.7904	68.8212	112.4773	96.7645	95.7364
6	119.4366	90.0741	89.8733	90.1582	104.7872	71.8194
7	0.0000	90.0825	89.8513	90.0394	99.8400	54.3089
8	90.0825	0.0000	92.8640	37.9341	93.6165	93.2392
9	89.8513	92.8640	0.0000	104.0881	90.5053	90.7533
10	90.0394	37.9341	104.0881	0.0000	94.2277	93.5884
11	99.8400	93.6165	90.5053	94.2277	0.0000	90.4336
12	54.3089	93.2392	90.7533	93.5884	90.4936	0.0000

TABLE XIV

Angle Matrix with 20% Mass Change

	1	2	3	4	5	6
1	0.0000	89.9883	89.9986	90.0076	90.8951	124.0894
2	89.9863	0.0000	65.2012	174.8062	116.6249	90.0492
3	89.9988	65.2012	0.0000	118.1720	104.2001	89.5824
4	90.0076	174.8065	118.1720	0.0000	60.6928	89.9576
5	90.0951	116.6249	104.2001	60.6928	0.0000	89.6903
6	124.0894	90.0492	89.9824	89.9576	89.6903	0.0000
7	71.6635	90.0359	89.9628	89.9772	90.0010	120.1351
8	90.0400	108.2412	115.9570	71.5885	102.8423	90.0760
9	90.0156	117.1463	91.9086	65.9119	69.0926	89.8745
10	89.9948	88.8619	80.1204	92.8619	113.0416	90.1624
11	139.6665	92.3373	90.5802	87.2966	83.0830	75.3050
12	83.6862	87.7259	89.2556	92.5902	95.8572	70.4391

	7	8	9	10	11	12
1	71.6635	90.0400	90.0156	89.9949	139.6665	83.6862
2	90.0365	108.2412	117.1463	88.8619	92.3373	87.7259
3	89.9628	115.9570	91.9096	80.1204	90.5802	89.2556
4	89.9772	71.5885	65.9119	92.0619	87.2966	92.5902
5	90.0010	102.8423	69.0926	113.0416	83.0830	95.8572
6	120.1351	90.0760	89.8745	90.1624	75.3050	70.4391
7	0.0000	90.0755	89.8518	90.0362	79.8297	56.4074
8	90.0755	0.0000	91.8593	37.9764	86.2731	93.3463
9	89.8518	91.8593	0.0000	104.9249	89.5103	90.7575
10	90.0362	37.9764	104.9249	0.0000	85.6344	93.6457
11	79.8297	86.2731	89.5103	85.6944	0.0000	88.9311
12	56.4074	93.3463	90.7575	93.6457	88.9311	0.0000

TABLE XV

Angle Matrix with Mass Proportion Change

	1	2	3	4	5	6
1	0.0000	89.9876	89.9991	90.0088	90.0885	56.6687
2	89.9876	0.0000	67.9385	175.4363	116.9616	89.9447
3	89.9991	67.9385	0.0000	114.7622	103.8782	90.0138
4	90.0088	175.4363	114.7622	0.0000	60.5714	90.0495
5	90.0885	116.9616	103.8782	60.5714	0.0000	90.3092
6	56.6687	99.9447	90.1328	90.0495	90.3092	0.0000
7	72.3954	90.0351	89.9620	89.9773	89.9845	61.1721
8	90.1492	106.3473	116.6995	73.4728	102.7894	89.9300
9	90.0129	116.3590	91.3043	66.3991	69.1853	90.1267
10	90.0061	88.2308	79.9539	92.3968	112.6655	89.8403
11	140.9311	91.9666	90.5957	87.6792	83.4320	104.8729
12	80.6971	88.0763	89.2928	92.2303	95.5756	105.9443

	7	8	9	10	11	12
1	72.3954	90.0492	90.0129	90.0061	140.9311	80.6971
2	90.0351	106.3473	116.3590	88.2308	91.9666	88.0763
3	89.9620	116.6995	91.3043	79.9539	90.5957	89.2928
4	89.9773	73.4728	66.3990	92.3958	87.6792	92.2303
5	89.9845	102.7894	69.1853	112.6655	83.4320	95.5756
6	61.1721	89.9300	90.1267	89.8403	104.8729	105.9443
7	0.0000	90.0886	89.8484	90.0523	80.7988	51.4492
8	90.0886	0.0000	92.3421	39.1026	86.5713	93.0572
9	89.8484	92.3421	0.0000	105.7099	89.7266	90.5322
10	90.0523	39.1026	105.7099	0.0000	85.9199	93.4492
11	80.7988	86.5713	89.7266	85.9199	0.0000	90.4827
12	51.4492	93.0572	90.5322	93.4492	90.4827	0.0000

TABLE XVI

Angle Matrix with Equal Mass Corners

	1	2	3	4	5	6
1	0.0000	89.9880	89.9988	90.0081	90.0946	123.2426
2	89.9880	0.0000	65.7677	175.0560	116.6448	90.0466
3	69.9988	65.7677	0.0000	117.3911	104.4288	89.9820
4	90.0081	175.0560	117.3911	0.0000	60.7695	89.9596
5	90.0946	116.6448	104.4288	60.7695	0.0000	89.6890
6	123.2426	90.0466	89.9820	89.9596	89.6890	0.0000
7	72.3479	90.0355	89.9619	89.9762	89.9951	119.5189
8	90.0471	108.2480	114.3825	71.7586	102.6075	90.0740
9	90.0147	116.6529	91.6308	66.2921	69.4423	89.8772
10	89.9984	84.3437	79.9181	96.0198	114.6969	90.1752
11	40.4695	88.0756	89.3477	92.3070	96.6715	104.6088
12	83.0063	88.0505	88.2420	92.2379	95.6539	70.8076

	7	8	9	10	11	12
1	72.3479	90.0471	90.8147	89.9984	40.4695	83.0063
2	90.0355	108.2480	116.6529	84.3437	88.0756	88.8905
3	89.9619	114.3825	91.6308	79.6181	89.3477	89.2420
4	89.9762	71.7586	66.2921	96.0198	92.3070	92.2379
5	89.9951	102.6075	69.4423	114.6969	96.6715	95.6539
6	119.5189	90.0740	89.8772	90.1752	104.6089	70.8976
7	0.0000	90.0737	89.8516	90.0595	100.1910	55.3692
8	90.0737	0.0000	89.5405	41.7858	93.5619	93.1830
9	89.8516	89.5405	0.0000	113.1043	90.0662	90.3736
10	90.0595	41.7858	113.1043	0.0000	94.0219	83.3597
11	100.1910	93.5619	90.0662	84.0219	0.0000	90.8776
12	55.3692	93.1829	90.3736	93.3597	90.8773	0.0000

VI Conclusions and Recommendations

By separating the system matrix modes into orthogonal groups, the system will be inherently decoupled. It is apparent that the judicious choice of sensor/actuator location and orientation can achieve acceptable orthogonal groups. It is also obvious that a single misplaced sensor/actuator pair can destroy a previous modal grouping set. The practical result is that modal groups can only be partially decoupled because of the difficulty in finding the ideal sensor/actuator model.

The attempts to decouple modes 11 and 12 show the ease with which a single coupling angle can be changed. However, the difficulties in finding an orientation that will change only one angle and leave the others unchanged was also demonstrated. The problem of trying to improve all coupling characteristics can only be solved by concentrating on improving one angle at a time. By this method, a systematic study should produce the desired sensor/actuator model.

The studies of the mass model changes showed little effect on the modal angles.

The next step in the study of sensor/actuator placement should be that of more modes. In this study, twelve modes are separated into groups. The methods of this study can be applied to a larger number of modes. However, a more rigorous method of determining the modal groupings needs to be made.

A possible method is a variation of the method that ORIENT uses (requirements of acceptance). The angle matrix could be inputed into a program that would output possible groupings based on

some given criteria. This criteria would be similar to that used in ORIENT; all angles coupled within some limit would be in the same group and those angles decoupled would be in different groups. The angles that don't fit the criteria would be listed as problem angles for each grouping. These angles would then be subject to correction using ORIENT.

I feel that the conditions of changing one angle without changing any other angle needs to be studied. If it can be determined when this condition is applicable, it will be a powerful tool. This method could be applied to every angle until all groups were perfect. Implementation of this method would be in ORIENT's requirements of acceptance.

One other step needs to be taken: experimental evaluation. The case in controlling a structure, when an added sensor/actuator improves the modal groups' coupling, can be studied experimentally. Thus, once a sensor/actuator model is found to be acceptable, it can be tested to see if it is experimentally acceptable.

Bibliography

1. "ACOSS FIVE (Active Control of Space Structures) Phase IA," LMSC Final Technical Report, RADC-TR-82-21, March 1982.

2. Calico, R. A., Jr., and Janiszewski, A. M., "Control of a Flexible Satellite Via Elimination of Control Spillover," Proceeds Third VPI/AIAA Symposium on Large Space Structures, Blacksburg, Virginia, June 1981.

3. Calico, R. A., Jr., and Miller, W. T., "Decentralized Control of Large Space Structures," Air Force Institute of Technology, Dayton, Ohio, December 1981.

4. Cook, R. D., "Concepts and Applications of Finite Element Analysis," Second Edition, New York: John Wiley & Sons, 1981.

5. Henderson, T., "VCOSS Design Model and Disturbances," Charles Stark Draper Laboratory, Cambridge, Massachusetts, November 1981.

6. Henderson, T., "Active Control of Space Structures (ACOSS) Model 2," Charles Stark Draper Laboratory Report C-5437, September 1981.

Appendix A

NASTRAN Data Deck

The listing below is the NASTRAN Data Deck for the CSDL II, Revision 3 large space structure. Cards of interest are: EIGR, GRID, CBAR, CONM2 and PBAR.

The input data card EIGR stands for Real Eigenvalue Extraction Data. The method used is the inverse power (INV) method with symmetric matrices. The frequency range of the eigenvalues is given with the next two numbers, 0-14hz. The estimate of the number of eigenvalues in the frequency range is given next, while the following number asks that all the eigenvalues be given.

GRID is the input card which defines the location of all the nodes of the model. This card is very useful in determining differences between similar models.

The CBAR card is Simple Beam Element Connection. This card identifies each bar element, and gives the nodes that are connected to its ends.

CONM2 is the card that was varied in this investigation. It stands for Concentrated Mass Element Connection. This card allows lumped masses to be put at the nodes. The mass to be changed is the third number on the card. On some of the cards, the moments of inertia are also given following the lumped mass.

Simple Beam Properties are listed in PBAR. The properties listed are: area, moments of inertia, and the torsional constant. This card could have been used to alter any of the properties of the mirror support trusses.

```
ID DRAPER,MODEL2
APP DISP
SCL 3
TIME 60
CEND
TITLE = ACOSS MODEL #2  - REVISION 3
SUBTITLE = VCOSS DESIGN MODEL
LABEL = 156 MODES AND FREQUENCIES
MPC = 100
METHOD = 600
DISP(PRINT,PUNCH) = ALL
SESE = ALL
BEGIN BULK
PARAM   GRDPNT  0
EIGR    600     INV     0.0     10.0    40      40                      1.0 E-03+10
+10     MASS
$
$       KINEMATIC MOUNT:  TERTIARY MIRROR
$
CRIGD3  1003    27      123     29      23      3233    3               +RB31
+RB31   MSET    1003    123456
$
$       KINEMATIC MOUNT:  PRIMARY MIRROR
$
CRIGD3  1001    34      123     35      23      2830    3               +RB11
+RB11   MSET    1001    123456
$
$       KINEMATIC MOUNT:  FOCAL PLANE
$
CRIGD3  1004    11      123     9       23      40      3               +RB41
+RB41   MSET    1004    123456
$
$       KINEMATIC MOUNT:  SECONDARY MIRROR
$
CRIGD3  1002    910     123     1112    23      40      3               +RB21
+RB21   MSET    1002    123456
$
$         IGID EQUIPMENT SECTION
$
CRIGD1  141     44      42      43      45      46      47
$
$    NODE POINT LOCATIONS
$       NODE#                   X (M)   Y (M)   Z (M)
$
GRID    1                       -7.0    0.0     0.0
GRID    2                       -4.0    5.0     0.0
GRID    3                       -4.0    -5.0    0.0
GRID    4                       0.0     5.0     0.0
GRID    5                       4.0     5.0     0.0
GRID    6                       4.0     -5.0    0.0
GRID    7                       7.0     0.0     0.0
GRID    8                       -7.0    0.0     2.0
GRID    9                       -4.0    5.0     2.0
GRID    1004                    0.0     4.0     2.0
GRID    10                      -4.0    -5.0    2.0
GRID    11                      4.0     5.0     2.0
GRID    12                      4.0     -5.0    2.0
GRID    910                     -4.0    -2.5    2.0
GRID    1112                    4.0     -2.5    2.0
GRID    13                      7.0     0.0     2.0
GRID    14                      -6.0    0.0     12.
GRID    15                      -4.0    4.0     12.
GRID    16                      -4.0    -4.0    12.
GRID    17                      4.0     4.0     12.
```

```
GRID    18              4.0     -4.0    12.
GRID    19              6.0     0.0     12.0
GRID    26              -5.0    0.0     22.0
GRID    27              -4.0    3.0     22.0
GRID    28              -4.0    -3.0    22.0
GRID    2830            0.0     -3.0    22.0
GRID    1001            0.0     -6.5    22.0
GRID    29              4.0     3.0     22.0
GRID    30              4.0     -3.0    22.0
GRID    31              5.0     0.0     22.0
GRID    32              -4.0    10.0    22.0
GRID    3233            0.0     10.0    22.0
GRID    1003            0.0     6.5     22.0
GRID    33              4.0     10.0    22.0
GRID    34              -4.0    -10.0   22.0
GRID    35              4.0     -10.0   22.0
GRID    36              -4.0    3.0     24.0
GRID    37              -4.0    -3.0    24.0
GRID    38              4.0     3.0     24.0
GRID    39              4.0     -3.0    24.0
GRID    40              0.0     2.5     2.0
GRID    1002            0.0     0.0     2.0
GRID    42              0.0     5.0     -0.3
GRID    43              -2.0    0.0     -1.3
GRID    44              0.0     -1.667  -1.3
GRID    45              2.0     0.0     -1.3
GRID    46              -4.0    -5.0    -0.3
GRID    47              4.0     -5.0    -0.3
GRID    48              -26.0   0.0     -1.3
GRID    49              -21.00  0.0     -1.3
GRID    50              -16.0   0.0     -1.3
GRID    51              -11.0   0.0     -1.3
GRID    52              -6.0    0.0     -1.3
GRID    53              6.0     0.0     -1.3
GRID    54              11.0    0.0     -1.3
GRID    55              16.0    0.0     -1.3
GRID    56              21.00   0.0     -1.3
GRID    57              26.0    0.0     -1.3
GRID    100             0.0     0.0     0.0             45
$
$     ELEMENT CONNECTION DATA
$
$      ELEM#    PROP#    NODE    NODE       LOCAL AXIS ORIENTATION VECTOR
$                         A       B
$
BAROR                                       1.0     0.0     0.0     1
CBAR     1       1        1       2
CBAR     2       2        1       3
CBAR     3       3        2       3
CBAR     4       4        2       4         0.0     1.0     0.0     1
CBAR     5       5        3       4
CBAR     6       6        4       5         0.0     1.0     0.0     1
CBAR     7       7        4       6
CBAR     8       8        3       5         0.0     1.0     0.0     1
CBAR     9       9        5       6
CBAR     10      10       5       7
CBAR     11      11       6       7
CBAR     12      12       1       8
CBAR     13      13       2       9
CBAR     14      14       3       10
CBAR     15      15       5       11
CBAR     16      16       6       12
CBAR     17      17       7       13
CBAR     18      18       3       8
CBAR     19      19       2       9
CBAR     21      21       4       9
```

CBAR	22	22	4	11				
CBAR	24	24	5	13				
CBAR	25	25	6	13				
CBAR	26	26	1112	3				
CBAR	27	27	6	10				
CBAR	30	30	5	9				
CBAR	31	31	8	10				
CBAR	32	32	9	910				
CBAR	232	232	910	10				
CBAR	33	33	9	40				
CBAR	34	34	910	40				
CBAR	35	35	11	40				
CBAR	36	36	1112	40				
CBAR	37	37	9	11	0.0	1.0	0.0	1
CBAR	38	38	10	12	0.0	1.0	0.0	1
CBAR	39	39	11	1112				
CBAR	239	239	1112	12				
CBAR	201	201	910	1112	0.0	1.0	0.0	1
CBAR	202	202	2	910				
CBAR	203	203	3	910				
CBAR	204	204	5	1112				
CBAR	205	205	6	1112				
CBAR	207	207	12	910				
CBAR	40	40	11	13				
CBAR	41	41	12	13				
CBAR	42	42	14	15				
CBAR	43	43	14	16				
CBAR	44	44	16	15				
CBAR	45	45	17	19				
CBAR	46	46	17	19				
CBAR	47	47	19	19				
CBAR	54	54	26	27				
CBAR	55	55	26	28				
CBAR	56	56	27	28				
CBAR	57	57	29	30				
CBAR	58	56	29	31				
CBAR	59	59	30	31				
CBAR	60	60	27	29	0.0	1.0	0.0	1
CBAR	61	61	27	30				
CBAR	62	62	28	2830	0.0	1.0	0.0	1
CBAR	194	184	2830	30	0.0	1.0	0.0	1
CBAR	63	63	27	36				
CBAR	64	64	28	37				
CBAR	65	65	30	39				
CBAR	66	66	29	38				
CBAR	67	67	29	36				
CBAR	68	68	27	37				
CBAR	69	69	28	39				
CBAR	70	70	30	35				
CBAR	71	71	36	37				
CBAR	72	72	37	39	0.0	1.0	0.0	1
CBAR	73	73	39	39				
CBAR	74	74	36	38	0.0	1.0	0.0	1
CBAR	75	75	37	38				
CBAR	127	127	26	37				
CBAR	128	128	26	36				
CBAR	129	129	31	39				
CBAR	130	130	31	38				
CBAR	76	76	8	14				
CBAR	77	77	10	14				
CBAR	78	78	13	16				
CBAR	79	79	16	9				
CBAR	80	80	9	15				
CBAR	181	181	9	15				
CBAR	182	182	6	40				
CBAR	183	183	2	40				

```
CBAR    186     186     3       40
CBAR    187     187     5       40
CBAR    81      81      11      17
CBAR    82      82      11      18
CBAR    83      83      12      18
CBAR    84      84      12      19
CBAR    85      85      13      19
CBAR    86      86      13      17
CBAR    87      87      14      26
CBAR    88      88      14      28
CBAR    89      89      16      28
CBAR    90      90      16      27
CBAR    91      91      15      27
CBAR    92      92      15      26
CBAR    93      93      17      29
CBAR    94      94      18      29
CBAR    95      95      18      30
CBAR    96      96      19      30
CBAR    97      97      19      31
CBAR    98      98      17      31
CBAR    99      99      15      32
CBAR    100     100     16      34
CBAR    101     101     17      33
CBAR    102     102     18      35
CBAR    111     111     26      32
CBAR    112     112     27      32
CBAR    113     113     27      33
CBAR    114     114     29      33
CBAR    115     115     31      33
CBAR    116     116     32      3233    0.0     1.0     0.0     1
CBAR    185     185     3233    33      0.0     1.0     0.0     1
CBAR    117     117     26      34
CBAR    118     118     28      34
CBAR    119     119     30      34
CBAR    120     120     30      35
CBAR    121     121     31      35
CBAR    122     122     34      35      0.0     1.0     0.0     1
CBAR    123     123     32      36
CBAR    124     124     33      38
CBAR    125     125     34      37
CBAR    126     126     35      39
CBAR    131     131     48      49      0.0     1.0     0.0     1
CBAR    132     132     49      50      0.0     1.0     0.0     1
CBAR    133     133     50      51      0.0     1.0     0.0     1
CBAR    134     134     51      52      0.0     1.0     0.0     1
CBAR    135     135     52      43      0.0     1.0     0.0     1
CBAR    136     136     45      53      0.0     1.0     0.0     1
CBAR    137     137     53      54      0.0     1.0     0.0     1
CBAR    138     138     54      55      0.0     1.0     0.0     1
CBAR    139     139     55      56      0.0     1.0     0.0     1
CBAR    140     140     56      57      0.0     1.0     0.0     1
$
$     ISOLATOR SPRINGS
$
$         ELEM#         K      NODE      DOF       NODE      DOF
$                     (N/M)     A         A         B         B
$
CELAS2  142     5.79E3  4       1       42      1
CELAS2  143     5.79E3  4       2       42      2
CELAS2  144     5.79E3  4       3       42      3
CELAS2  145     5.79E3  3       1       46      1
CELAS2  146     5.79E3  3       2       46      2
CELAS2  147     5.79E3  3       3       46      3
CELAS2  148     5.79E3  6       1       47      1
CELAS2  149     5.79E3  6       2       47      2
CELAS2  150     5.79E3  6       3       47      3
```

```
$
$     MATERIAL PROPERTY DATA
$
$        MAT#       E                NU       RHO
$
MAT1     100      1.24E+11         0.3      1720.
MAT1     200      1.24E+11         0.3      1720.
MAT1     300      1.24E+11         0.3      2579.70
$
$     LUMPED MASS DATA
$
$CONM2   ELEM#   NODE#            MASS                                  +XXX
$+XXXX     IXX            IYY                     IZZ
$
$       MIRRORS
$
CONM2    1001    1001             1000.                                 +100
+1001    4083.33         5333.33                  5416.67
CONM2    1002    1002             500.                                  +404
+4040    1666.67         4266.67                  5933.33
CONM2    1003    1003             1200.                                 +100
+1003    4900.           6400.                    11300.
CONM2    1004    1004             600.                                  +100
+1004    200.            500.                     1000.
$
$       EQUIPMENT SECTION
$
CONM2    544     44               3500.                                 +544
+544     20611.          10500.                   29777.
$
$     SOLAR PANELS
$
CONM2    548     48               81. 1                                 +548
+548     270.0
CONM2    550     50               163.62                                +550
+550     540.0
CONM2    552     52               73.62                                 +552
+552     270.0
CONM2    553     53               73.62                                 +553
+553     270.0
CONM2    557     57               81.91                                 +557
+555     540.0
CONM2    555     55               163.62                                +555
+557     270.0
$
$       ADDITIONAL NON-STRUCTURAL MASS AT MIRROR SUPPORTS
$
CONM2    501     27               69.5
CONM2    502     28               6.74
CONM2    503     29               59.5
CONM2    504     30               6.74
CONM2    505     32               6.74
CONM2    506     33               6.74
CONM2    507     34               59.5
CONM2    508     35               59.5
CONM2    509     9                67.4
CONM2    510     10               67.4
CONM2    511     11               67.4
CONM2    512     12               67.4
$
$       BEAM SECTION PROPERTIES
$
$PBAR                  PROP#  MAT#                 AREA            I11      +XXX
$+XXXXXXX          I22             J
$
PBAR*                    1    100             0.673543E-04     0.439721E-07*
```

•	1	0.439721E-07	0.679442E-07		
PBAR•	2	100		0.678583E-04	0.439721E-07•
•	2	0.439721E-07	0.679442E-07		
PBAR•	3	100		0.255096E-03	0.621422E-06•
•	3	0.621422E-06	0.124284E-05		
PBAR•	4	100		0.678583E-04	0.439721E-07•
•	4	0.439721E-07	0.679443E-07		
PBAR•	5	100		0.343532E-03	0.112695E-05•
•	5	0.112695E-05	0.225391E-05		
PBAR•	6	100		0.678583E-04	0.439721E-07•
•	6	0.439721E-07	0.679443E-07		
PBAR•	7	100		0.343532E-03	0.112695E-05•
•	7	0.112695E-05	0.2253 1E-05		
PBAR•		100		0.104152E-03	0.103587E-06•
•	8	0.103587E-06	0.207174E-06		
PBAR•	9	100		0.255098E-03	0.621422E-06•
•	9	0.621422E-06	0.124284E-05		
PBAR•	10	100		0.678583E-04	0.439721E-07•
•	10	0.439721E-07	0.679442E-07		
PBAR•	11	100		0.678583E-04	0.439721E-07•
•	11	0.439721E-07	0.679442E-07		
PBAR•	12	100		0.678583E-04	0.439721E-07•
•	12	0.439721E-07	0.679443E-07		
PBAR•	13	100		0.678583E-04	0.439721E-07•
•	13	0.439721E-07	0.679443E-07		
PBAR•	14	100		0.678583E-04	0.439721E-07•
•	14	0.439721E-07	0.679443E-07		
PBAR•	15	100		0.678583E-04	0.439721E-07•
•	15	0.439721E-07	0.679443E-07		
PBAR•	16	100		0.678583E-04	0.439721E-07•
•	16	0.439721E-07	0.679443E-07		
PBAR•	17	100		0.678583E-04	0.439721E-07•
•	17	0.439721E-07	0.679442E-07		
PBAR•	1	100		0.678583E-04	0.439721E-07•
•	1	0.439721E-07	0.679442E-07		
PBAR•	19	100		0.678583E-04	0.439721E-07•
•	19	0.439721E-07	0.679442E-07		
PBAR•	21	100		0.678583E-04	0.439721E-07•
•	21	0.439721E-07	0.679443E-07		
PBAR•	22	100		0.678583E-04	0.439721E-07•
•	22	0.439721E-07	0.679443E-07		
PBAR•	24	100		0.678583E-04	0.439721E-07•
•	24	0.439721E-07	0.679442E-07		
PBAR•	25	100		0.678583E-04	0.439721E-07•
•	25	0.439721E-07	0.679442E-07		
PBAR•	26	100		0.140494E-03	0.188450E-06•
•	26	0.188450E-06	0.376974E-06		
PBAR•	27	100		0.140494E-03	0.188450E-06•
•	27	0.188450E-06	0.37697 E-06		
PBAR•	3	100		0.678583E-04	0.439721E-07•
•	30	0.439721E-07	0.679442E-07		
PBAR•	31	100		0.678583E-04	0.439721E-07•
•	31	0.439721E-07	0.679442E-07		
PBAR•	32	100		0.304583E-04	0.618177E-07•
•	32	0.618177E-07	0.123635E-06		
PBAR•	33	100		0.678583E-04	0.439721E-07•
•	33	0.439721E-07	0.679443E-07		
PBAR•	34	100		0.678583E-04	0.439721E-07•
•	34	0.439721E-07	0.679443E-07		
PBAR•	35	100		0.678583E-04	0.439721E-07•
•	35	0.439721E-07	0.679443E-07		
PBAR•	36	100		0.678583E-04	0.439721E-07•
•	36	0.439721E-07	0.679443E-07		
PBAR•	37	100		0.104152E-03	0.103587E-06•
•	37	0.103587E-06	0.207174E-06		
PBAR•	3-	100		0.104152E-03	0.103587E-06•

•	38	0.103587E-06	0.207174E-06		
PBAR•	39	100		0.694593E-04	0.618177E-07•
•	39	0.618177E-07	0.123635E-06		
PBAR•	40	100		0.679583E-04	0.439721E-07•
•	40	0.439721E-07	0.879442E-07		
PBAR•	41	100		0.679583E-04	0.439721E-07•
•	41	0.439721E-07	0.879442E-07		
PBAR•	42	100		0.679583E-04	0.439721E-07•
•	42	0.439721E-07	0.879443E-07		
PBAR•	43	100		0.679583E-04	0.439721E-07•
•	43	0.439721E-07	0.879443E-07		
PBAR•	44	100		0.104152E-03	0.103587E-06•
•	44	0.103587E-06	0.207174E-06		
PBAR•	45	100		0.104152E-03	0.103587E-06•
•	45	0.103587E-06	0.207174E-06		
PBAR•	46	100		0.679583E-04	0.439721E-07•
•	46	0.439721E-07	0.879443E-07		
PBAR•	47	100		0.679583E-04	0.439721E-07•
•	47	0.439721E-07	0.879443E-07		
PBAR•	54	100		0.679583E-04	0.439721E-07•
•	54	0.439721E-07	0.879442E-07		
PBAR•	55	100		0.679583E-04	0.439721E-07•
•	55	0.439721E-07	0.879442E-07		
PBAR•	56	100		0.679583E-04	0.439721E-07•
•	56	0.439721E-07	0.879442E-07		
PBAR•	57	100		0.679583E-04	0.439721E-07•
•	57	0.439721E-07	0.879442E-07		
PBAR•	58	100		0.679583E-04	0.439721E-07•
•	58	0.439721E-07	0.879442E-07		
PBAR•	59	100		0.679583E-04	0.439721E-07•
•	59	0.439721E-07	0.879442E-07		
PBAR•	60	100		0.104152E-03	0.103587E-06•
•	60	0.103587E-06	0.207174E-06		
PBAR•	61	100		0.255098E-03	0.621422E-06•
•	61	0.621422E-06	0.124284E-05		
PBAR•	62	300		0.0060921	0.0015205 •
•	62	0.0015205	0.0030410		
PBAR•	63	100		0.679583E-04	0.439721E-07•
•	63	0.439721E-07	0.879443E-07		
PBAR•	64	100		0.679583E-04	0.439721E-07•
•	64	0.439721E-07	0.879443E-07		
PBAR•	65	100		0.679583E-04	0.439721E-07•
•	65	0.439721E-07	0.879443E-07		
PBAR•	66	100		0.679563E-04	0.439721E-07•
•	66	0.439721E-07	0.879443E-07		
PBAR•	67	100		0.117640E-03	0.132154E-06•
•	67	0.132154E-06	0.26430[illegible]E-06		
PBAR•	68	100		0.679563E-04	0.439721E-07•
•	68	0.439721E-07	0.879442E-07		
PBAR•	69	100		0.117640E-03	0.132154E-06•
•	69	0.132154E-06	0.26430[illegible]E-06		
PBAR•	70	100		0.679563E-04	0.439721E-07•
•	70	0.439721E-07	0.879442E-07		
PBAR•	71	100		0.679583E-04	0.439721E-07•
•	71	0.439721E-07	0.879442E-07		
PBAR•	72	100		0.104152E-03	0.103587E-06•
•	72	0.103587E-06	0.207174E-06		
PBAR•	73	100		0.679583E-04	0.439721E-07•
•	73	0.439721E-07	0.879442E-07		
PBAR•	74	100		0.104152E-03	0.103587E-06•
•	74	0.103587E-06	0.207174E-06		
PBAR•	75	100		0.255098E-03	0.621422E-06•
•	75	0.621422E-06	0.124284E-05		
PBAR•	76	100		0.259503E-03	0.643065E-06•
•	76	0.643065E-06	0.128613E-05		
PBAR•	77	100		0.424114E-03	0.171755E-05•

•	77	0.171765E-05	0.343531E-05		
PBAR•		78	100	0.259503E-03	0.643065E-06•
•	78	0.643065E-06	0.128613E-05		
PBAR•		79	100	0.833904E-03	0.664055E-05•
•	79	0.664055E-05	0.132811E-04		
PBAR•		80	100	0.259503E-03	0.643065E-06•
•	80	0.643065E-06	0.128613E-05		
PBAR•		81	100	0.259503E-03	0.643065E-06•
•	81	0.643065E-06	0.128613E-05		
PBAR•		82	100	0.833904E-03	0.664055E-05•
•	82	0.664055E-05	0.132811E-04		
PBAR•		83	100	0.259503E-03	0.643065E-06•
•	83	0.643065E-06	0.128613E-05		
PBAR•		84	100	0.424114E-03	0.171765E-05•
•	84	0.171765E-05	0.343531E-05		
PBAR•		85	100	0.259503E-03	0.643065E-06•
•	85	0.643065E-06	0.128613E-05		
PBAR•		86	100	0.391135E-03	0.151367E-05•
•	86	0.151367E-05	0.302735E-05		
PBAR•		87	100	0.259503E-03	0.643065E-06•
•	87	0.643065E-06	0.128613E-05		
PBAR•		88	100.	0.325124E-03	0.100942E-05•
•	88	0.100942E-05	0.201883E-05		
PBAR•		89	100	0.259503E-03	0.643065E-06•
•	89	0.643065E-06	0.128613E-05		
PBAR•		90	100	0.566323E-03	0.306267E-05•
•	90	0.306267E-05	0.612533E-05		
PBAR•		91	100	0.259503E-03	0.643065E-06•
•	91	0.643065E-06	0.128613E-05		
PBAR•		92	100	0.349640E-03	0.116072E-05•
•	92	0.116072E-05	0.232143E-05		
PBAR•		93	100	0.259503E-03	0.643065E-06•
•	93	0.643065E-06	0.128613E-05		
PBAR•		94	100	0.566323E-03	0.306267E-05•
•	94	0.306267E-05	0.612533E-05		
PBAR•		95	100	0.259503E-03	0.643065E-06•
•	95	0.643065E-06	0.128613E-05		
PBAR•		96	100	0.325124E-03	0.100942E-05•
•	96	0.100942E-05	0.201883E-05		
PBAR•		97	100	0.259503E-03	0.643065E-06•
•	97	0.643065E-06	0.128613E-05		
PBAR•		98	100	0.349640E-03	0.116072E-05•
•	98	0.116072E-05	0.232143E-05		
PBAR•		99	100	0.470559E-03	0.211446E-05•
•	99	0.211446E-05	0.422892E-05		
PBAR•		100	100	0.470559E-03	0.211446E-05•
•	100	0.211446E-05	0.422892E-05		
PBAR•		101	100	0.470559E-03	0.211446E-05•
•	101	0.211446E-05	0.422892E-05		
PBAR•		102	100	0.470559E-03	0.211446E-05•
•	102	0.211446E-05	0.422892E-05		
PBAR•		111	100	0.259503E-03	0.643065E-06•
•	111	0.643065E-06	0.128613E-05		
PBAR•		112	100	0.678583E-04	0.439721E-07•
•	112	0.439721E-07	0.879443E-07		
PBAR•		113	100	0.325124E-03	0.100942E-05•
•	113	0.100942E-05	0.201883E-05		
PBAR•		114	100	0.678583E-04	0.439721E-07•
•	114	0.439721E-07	0.879443E-07		
PBAR•		115	100	0.259503E-03	0.643065E-06•
•	115	0.643065E-06	0.128613E-05		
PBAR•		116	300	0.0060921	0.0015205 •
•	116	0.0015205	0.0030410		
PBAR•		117	100	0.259503E-03	0.643065E-06•
•	117	0.643065E-06	0.128613E-05		
PBAR•		118	100	0.678583E-04	0.439721E-07•

• 118	0.439721E-07	0.879443E-07	PBAR•	119	100	0.325124E-03	0.100942E-05•
• 119	0.100942E-05	0.201863E-05	PBAR•	120	100	0.678583E-04	0.439721E-07•
• 120	0.439721E-07	0.879443E-07	PBAR•	121	100	0.252503E-03	0.643065E-06•
• 121	0.643065E-06	0.128613E-05	PBAR•	122	100	0.104152E-03	0.103567E-06•
• 122	0.103567E-06	0.207174E-06	PBAR•	123	100	0.716806E-04	0.490653E-07•
• 123	0.490653E-07	0.981305E-07	PBAR•	124	100	0.716806E-04	0.490653E-07•
• 124	0.490653E-07	0.981305E-07	PBAR•	125	100	0.716806E-04	0.490653E-07•
• 125	0.490653E-07	0.981305E-07	PBAR•	126	100	0.716806E-04	0.490653E-07•
• 126	0.490653E-07	0.981305E-07	PBAR•	127	100	0.675583E-04	0.439721E-07•
• 127	0.439721E-07	0.879443E-07	PBAR•	128	100	0.678583E-04	0.439721E-07•
• 128	0.439721E-07	0.879443E-07	PBAR•	129	100	0.678583E-04	0.439721E-07•
• 129	0.439721E-07	0.879443E-07	PBAR•	130	100	0.678583E-04	0.439721E-07•
• 130	0.439721E-07	0.879443E-07	PBAR•	131	100	6.107256E-04	3.561752E-06•
• 131	3.561752E-06	7.123504E-06	PBAR•	132	100	6.107256E-04	3.561752E-06•
• 132	3.561752E-06	7.123504E-06	PBAR•	133	100	6.107256E-04	3.561752E-06•
• 133	3.561752E-06	7.123504E-06	PBAR•	134	100	6.107256E-04	3.561752E-06•
• 134	3.561752E-06	7.123504E-06	PBAR•	135	100	6.107256E-04	3.561752E-06•
• 135	3.561752E-06	7.123504E-06	PBAR•	13-	100	6.107256E-04	3.561752E-06•
• 136	3.561752E-06	7.123504E-06	PBAR•	137	100	6.107256E-04	3.561752E-06•
• 137	3.561752E-06	7.123504E-06	PBAR•	13	100	6.107256E-04	3.561752E-06•
• 138	3.561752E-06	7.123504E-06	PBAR•	139	100	6.107256E-04	3.561752E-06•
• 139	3.561752E-06	7.123504E-06	PBAR•	14	100	6.107256E-04	3.561752E-06•
• 140	3.561752E-06	7.123504E-06	PBAR•	181	100	0.398135E-03	0.151367E-05•
• 191	0.151367E-05	0.302735E-05	PBAR•	192	100	0.343532E-03	0.112695E-05•
• 192	0.112695E-05	0.225391E-05	PBAR•	183	100	0.343532E-03	0.112695E-05•
• 183	0.112695E-05	0.225391E-05	PBAR•	194	300	0.0060921	0.0015205 •
• 194	0.0015205	0.0030410	PBAR•	195	300	0.0060921	0.0015205 •
• 135	0.0015205	0.0030410	PBAR•	186	100	0.343532E-03	0.112695E-05•
• 136	0.112695E-05	0.225391E-05	PBAR•	137	100	0.343532E-03	0.112695E-05•
• 137	0.112695E-05	0.225391E-05	PBAR•	201	100	0.104620E-03	0.104520E-06•
• 201	0.104520E-06	0.209040E-06	PBAR•	202	100	0.923628E-04	0.814640E-07•
• 202	0.814640E-07	0.162928E-06	PBAR•	203	100	0.678583E-04	0.439721E-07•
• 203	0.439721E-07	0.879442E-07	PBAR•	204	100	0.923628E-04	0.814640E-07•

```
*     204      0.814640E-07     0.162928E-06
PBAR*                   205    100                   0.678583E-04      0.439721E-07*      207
*     205      0.439721E-07     0.879442E-07
PBAR*                   207    100                   0.140494E-03      0.168490E-06*      207
*     207      0.168490E-06     0.376597 E-06
PBAR*                   232    100                   0.678583E-04      0.439721E-07*      232
*     232      0.439721E-07     0.-79442E-07
PBAR*                   23 100                       0.678583E-04      0.439721E-07*      233
*     233      0.439721E-07     0.879442E-07
$
$       MULTI-POINT CONSTRAINT EQUATION FOR X-AXIS LOS ERROR (NODE 100 DOF 1)
$
MPC*    100                            100                   1                -1.0*1000000
*1000000              34                  2  -0.01855287570                    *1000001
*1000001                                 34                  3  -0.14285714286*1000002
*1000002              35                  2  -0.01855287571                    *1000003
*1000003                                 35                  3  -0.14285714286*1000004
*1000004            2830                  3   0.28571428572                    *1000005
*1000005                                 30                  3   0.0           *1000006
*1000006              27                  2   0.08065681399                    *1000007
*1000007                                 27                  3  -0.35489000795*1000008
*1000008              29                  2   0.08065681399                    *1000009
*1000009                                 29                  3  -0.35489000795*1000010
*1000010            3233                  3   0.70978001590                    *1000011
*1000011                                 33                  3   0.0           *1000012
*1000012            1002                  4  -3.49423005566                    *1000013
*1000013                                 11                  2  -0.06210354429*1000014
*1000014                                  2  -0.06210354429
$
$       MULTI-POINT CONSTRAINT EQUATION FOR Y-AXIS LOS ERROR (NODE 100 DOF 2)
$
MPC*    100                            100                   2                -1.0*2000000
*2000000              34                  1  -0.03710575139                    *2000001
*2000001                                 34                  2  -0.24636219924*2000002
*2000002              34                  3  -0.25000000000                    *2000003
*2000003                                 35                  2   0.24636218924*2000004
*2000004              35                  3   0.25000000000                    *2000005
*2000005                                 27                  1   0.16131363995*2000006
*2000006              27                  2  -0.06049261499                    *2000007
*2000007                                 27                  3  -0.62105751391*2000008
*2000008               2                  2   0.06049261499                    *2000009
*2000009                                 29                  3   0.62105751391*2000010
*2000010            1002                  5   3.49423005566                    *2000011
*2000011                                 11                  1  -0.12420708859*2000012
*2000012              11                  2  -0.07762953037                    *2000013
*2000013                                  9                  2   0.07762953037*2000014
*2000014
$
$       MULTI-POINT CONSTRAINT EQUATION FOR DEFOCUS (NODE 100 DOF 3)
$
MPC*    100                            100                   3                -1.0*3000000
*3000000              34                  3  -0.01912393776                    *3000001
*3000001                                 35                  3  -0.01912393776*3000002
*3000002            2830                  3   0.12749291836                    *3000003
*3000003                                 30                  3   0.0           *3000004
*3000004              27                  3   0.77803217347                    *3000005
*3000005                                 29                  3   0.77803217347*3000006
*3000006            3233                  3  -0.46681930409                    *3000007
*3000007                               1002                  3  -0.17649008571*3000008
*3000008               9                  3   0.50000000000                    *3000009
*3000009                                 11                  3   0.50000000000*3000010
*3000010              40                  3  -2.00000000000
$
$       RIGID BODY SUPPORT
$
SUPORT  44       123456
```

Appendix B

SELECT

This program was used to pick off the critical modes from the eigenvectors obtained from NASTRAN. The input is read from TAPE 5, and the output (critical eigenvectors) is listed on TAPE 6.

The input file contains three pieces of information. First, the number of critical modes (N). Second, the list of eigenvector numbers (ID), and lastly, the 38 eigenvalues and eigenvectors. The output from NASTRAN needs to be modified so that only the eigenvectors and eigenvalues are present.

The eigenvectors are placed into a three dimensional array, MAT (59, 6, 38). The desired eigenvectors are then written into TAPE 6 using the ID vector to identify the critical ones.

Following is a description of the variables used in SELECT:

ID (I)	=	The eigenvector numbers of the critical modes.
M	=	Index, set equal to ID for each mode.
MAT(I,J,K)	=	Three dimensional array of eigenvectors.
MODE (K)	=	List of eigenvector numbers.
N	=	Number of critical modes.

```
      PROGRAM SELECT(INPUT,OUTPUT,TAPE5,TAPE6)
      DIMENSION MAT(59,6,38),MODE(38),ID(38)
      READ(5,*)N
      READ(5,*)(ID(I),I=1,N)
      DO 1 K=1,38
      READ(5,100)MODE(K)
      READ(5,200)((MAT(I,J,K),J=1,6),I=1,59)
    1 CONTINUE
      DO 2 K=1,N
      M=ID(K)
      WRITE(6,300)((MAT(I,J,M),J=1,6),I=1,59)
    2 CONTINUE
      PRINT*,"MODES READ ARE : ",(MODE(I),I=1,38)
      PRINT*,"MODES FILED ARE : ",(ID(I),I=1,N)
  100 FORMAT(I3)
  200 FORMAT(1P3E15.6)
  300 FORMAT(1X,1P3E15.6)
      END
```

Appendix C

ANGLE

This program uses the sensor/actuator model and the critical modes to calculate the system matrices (B and C), and the coupling angles between the system modes.

The program first reads the sensor/actuator model. The number of critical modes (N), actuators (NA), and sensors (NS) are read as integers. Next the orientation angles of the actuators ALPHA, BETA, and GAMMA are read. The identities of the nodes where the actuators are placed are listed in NODE. Note that this array allows multiple actuators at one node. The sensors are similarly read.

The critical modes are read next into PHI. To find the value corresponding to a particular node's degree of freedom, the ID vector is used. This vector orders the nodes of the structure:

ID (1-19)=1-19	ID (52)=910	ID(56)=1004
ID(20-34)=26-40	ID(53)=1001	ID(57)=1112
ID(35-50)=42-57	ID(54)=1002	ID(58)=2830
ID(51)=100	ID(55)=1003	ID(59)=3233

The calculation of the system matrices uses the formulas given in the text for elements of B and C. The only complication involves picking out the proper element of the eigenvector. This is accomplished using NODE and ID. NODE identifies the node in question, while ID translates this identification to determine which of the 59 nodes it is. This determination allows the proper PHI value to be picked out.

After the system matrices are calculated, it is a simple matter to determine the angles between the modes. The dot product formula given in the text is used to make the calculations. The norms squared of the rows (B) and columns (C) are given by BSQ and CSQ respectively. Dot products are CB and CC. The angles are put into matrices ANGB and ANGC.

Following is a description of the variables used in ANGLE:

ALPHA (I)	=	α , the angle between +x axis and the actuator.
ALPHS (I)	=	α, the angle between +x axis and the sensor.
ANGB (I,J)	=	The output matrix of angles between the rows of B.
ANGC (I,J)	=	The output matrix of angles between the columns of C.
B (I,J)	=	System matrix which is the ϕ matrix times the direction cosine matrix of the actuators.
BETA (I)	=	β, the angle between +y axis and the actuator.
BETS (I)	=	β, the angle between +y axis and the sensor.
BSQ (I)	=	The sum of the squares of each element in a row of B.
C (I,J)	=	System matrix which is the direction cosine matrix of the sensors times the ϕ matrix
CB	=	The dot product of two rows of B.
CC	=	The dot product of two columns of C.
CON	=	Conversion factor, $\pi/180$
CSQ (I)	=	The sum of the squares of each element in a column of C.
GAMMA (I)	=	γ, the angle between +z axis and the actuator.
GAMMS (I)	=	γ, the angle bestween +z axis and the sensor.

ID (I)	=	The node that corresponds to the rank number.
N	=	The number of critical modes.
NA	=	The number of actuators.
NODE (I)	=	The list of actuator nodes.
NODS (I)	=	The list of sensor nodes.
NS	=	The number of sensors
PHI (I J)	=	Input matrix of critical modes.
PI	=	π

```
      PROGRAM ANGLE(INPUT,OUTPUT,TAPE5,TAPE6)
      DIMENSION PHI(354,30),ALPHA(59),BETA(59),GAMMA(59)
      DIMENSION ALPHS(5 ),BETS(59),GAMMS(59),NODE(59),NODS(59),ID(5 )
      DIMENSION ANGB(30,30),ANGC(30,30),BSQ(59),CSQ(59)
      DIMENSION B(30,59),C(59,30)
      READ(5,*)N,NA,NS
      PRINT 200
      PRINT*," NUMBER OF CRITICAL MODES = ",N
      PRINT*," "
      PRINT*," NUMBER OF ACTUATOR  = ",NA
      PRINT*," "
      PRINT*," NUMBER OF SENSORS = ",NS
      READ(5,*)(ALPHA(I),I=1,NA)
      READ(5,*)(BETA(I),I=1,NA)
      READ(5,*)(GAMMA(I),I=1,NA)
      READ(5,*)(NODE(I),I=1,NA)
      PRINT*," "
      PRINT*," "
      PRINT*,"                  ORIENTATION OF ACTUATORS "
      PRINT*," "
      PRINT*,"    #        NODE      ALPHA       BETA      GAMMA "
      DO 1 I=1,NA
      PRINT*," "
    1 PRINT 300,I,NODE(I),ALPHA(I),BETA(I),GAMMA(I)
      READ(5,*)(ALPHS(I),I=1,NS)
      READ(5,*)(BETS(I),I=1,NS)
      READ(5,*)(GAMMS(I),I=1,NS)
      READ(5,*)(NODS(I),I=1,NS)
      PRINT*," "
      PRINT*," "
      PRINT*,"                  ORIENTATION OF SENSORS "
      PRINT*," "
      PRINT*,"    #        NODE      ALPHA       BETA      GAMMA "
      DO 2 I=1,NS
      PRINT*," "
    2 PRINT 300,I,NODS(I),ALPH (I),BETS(I),GAMMS(I)
      READ(5,400)((PHI(I,J),I=1,354),J=1,N)
      READ(5,*)(ID(I), =1,59)
      PI=3.14159265 0
      CON=PI/180.0
      DO 30 J=1,NA
      ALPHA(J)=ALPHA(J)*CON
      BETA(J)=BETA(J)*CON
      GAMMA(J)=GAMMA(J)*CON
      DO 10 K=1,59
   10 IF(ID(K).EQ.NODE(J))GO TO 20
   20 CONTINUE
      K=6*K-5
      DO 30 I=1,N
      B(I,J)=PHI(K,I)*COS(ALPHA(J))+PHI(K+1,I)*COS(BETA(J))
     1 +PHI(K+2,I)*COS(GAMMA(J))
   30 CONTINUE
```

```
      DO 60 I=1,NS
      ALPHS(I)=ALPHS(I)*CON
      BETS(I)=BETS(I)*CON
      GAMMS(I)=GAMMS(I)*CON
      DO 40 K=1,59
   40 IF(ID(K).EQ.NCDS(I))GO TO 50
   50 CONTINUE
      K=6*K-5
      DO 60 J=1,N
      C(I,J)=PHI(K,J)*COS(ALPHS(I))+PHI(K+1,J)*COS(BETS(I))
     1 +PHI(K+2,J)*COS(GAMMS(I))
   60 CONTINUE
      DO 70 I=1,N
      BSQ(I)=0.0
      DO 70 K=1,NA
      BSQ(I)=B(I,K)**2.0+BSQ(I)
   70 CONTINUE
      DO 90 I=1,N
      DO 90 J=1,N
      CB=0.0
      DO 80 K=1,NA
   80 CB=B(I,K)*B(J,K)+CB
      ANGB(I,J)=ACOS(CB/SQRT(BSQ(I))/SQRT(BSQ(J)))
      ANGB(I,J)=ANGB(I,J)/CON
   90 CONTINUE
      DO 100 I=1,N
      CSQ(I)=0.0
      DO 100 K=1,NS
      CSQ(I)=C(K,I)**2.0+CSQ(I)
  100 CONTINUE
      DO 120 I=1,N
      DO 120 J=1,N
      CC=0.0
      DO 110 K=1,NS
  110 CC=C(K,I)*C(K,J)+CC
      ANGC(I,J)=ACOS(CC/SQRT(CSQ(I))/SQRT(CSQ(J)))
      ANGC(I,J)=ANGC(I,J)/CON
  120 CONTINUE
      PRINT 200
      PRINT 203
      PRINT 210,(I,I=1,NA)
      DO 500 I=1,N
  500 PRINT 220,I,(B(I,J),J=1,NA)
      PRINT 200
      PRINT 204
      PRINT 210,(I,I=1,N)
      DO 600 I=1,NS
  600 PRINT 220,I,(C(I,J),J=1,N)
      PRINT 200
      PRINT 201
      PRINT 210,(I,I=1,N)
      DO 130 I=1,N
  130 PRINT 220,I,(ANGB(I,J),J=1,N)
```

```
      PRINT 200
      PRINT 202
      PRINT 210,(I,I=1,')
      DO 140 I=1,N
  140 PRINT 220,I,(ANGC(I,J),J=1,M)
  200 FORMAT(1H1)
  210 FORMAT(1X,5X,I7,11I10,/)
  220 FORMAT(1X,/,I5,12F10.4,/,5X,12F10.4)
  201 FORMAT(1X,20X,24HANGLES BETWEEN ROWS OF B)
  202 FORMAT(1X,20X,27HANGLES BETWEEN COLUMNS OF C)
  203 FORMAT(1X,20X,8HB MATRIX)
  204 FORMAT(1X,20X,8HC MATRIX)
  300 FORMAT(1X,I5,I11,F11.2,2F10.2)
  400 FORMAT(1P3E15.6)
      END
```

Appendix D

ORIENT

ORIENT is a modified ANGLE program used to calculate the angle matrix for many different actuator models. Two major differences between ANGLE and ORIENT exist. ORIENT has an added actuator that varies its location and orientation. It also has requirements of acceptance that give a measure of improvement.

ORIENT first calculates the B matrix without the added actuator. This part of the B matrix remains constant. Only a new column needs to be added with the new actuator. This new column is calculated for every node point and every possible orientation (step at 5^{o} increments).

After the new column is calculated, ANGB is determined as in ANGLE. However, after the angle is calculated for each mode pair, it is then tested. If any angle does not meet the requirements of acceptance, the program immediately steps to the next possible orientation for the actuator. If every angle meets the requirements, ANGB is printed out for the particular orientation and location of the actuator at that time.

This version of ORIENT establishes the requirements of acceptance by observing the coupling characteristics between the modes of different groups. The requirements differ depending on what groups the modes are in. If the modes are in the same group, they are required to be coupled. If they are in different groups, the angle has to indicate decoupling. This facet of the program is implemented by reading each mode number into a group (N1, N2, or N3) at the beginning of ORIENT.

This mode group identification allows great flexibility. First, a mode grouping can be tried by just assigning the modes to different groups. Second, the threshold for coupling and decoupling can be reassigned to any desired level. This is the method with which problem angles are dealt.

Following is a description of the variables used in ORIENT:

A	=	Possible α orientation, calculated at 5^o increments.
ALPHA (I)	=	α, the angle between +x axis and the actuator.
ANGB (I,J)	=	The output matrix of angles between the rows of B.
ARG	=	The cosine of the angle between the rows of B, argument of arc cosine equation.
B (I,J)	=	System matrix which is the ϕ matrix times the direction cosine matrix of the actuators.
BE	=	Possible β orientation, calculated at 5^o increments.
BETA (I)	=	β, the angle between +y axis and the actuator.
BSQ (I)	=	The sum of the squares of each element in a row of B.
CB	=	The dot product of two rows of B.
CON	=	Conversion factor, π /180.
G	=	Possible γ orientation, calculated from A and BE.
G2	=	180^o - G
GAMMA (I)	=	γ, the angle between +z axis and the actuator.
I1	=	Index of modes in group 1.
I2	=	Index of modes in group 2.
I3	=	Index of modes in group 3.

ID (I)	=	The node that corresponds to the rank number.
N	=	The number of critical modes.
N1 (I)	=	First group of modes.
N2 (I)	=	Second group of modes.
N3 (I)	=	Third group of modes.
NA	=	The number of actuators.
NAA	=	NA + 1.
ND	=	Index, set equal to ID for each node.
NODE (I)	=	The list of actuator nodes.
PHI (I,J)	=	Input matrix of critical modes.
PI	=	π

```
      PROGRAM ORIENT(INPUT,OUTPUT,TAPE5,TAPE6)
      DIMENSION PHI(354,30),ALPHA(59),BETA(59),GAMMA(59)
      DIMENSION NODE(59),ID(59),N1(5),N2(5),N3(5)
      DIMENSION ANGB(30,30),BSQ(59),B(30,59)
      READ(5,*)N,NA
      READ(5,*)(N1(I),I=1,4)
      READ(5,*)(N2(I),I=1,5)
      READ(5,*)(N3(I),I=1,3)
      PRINT 200
      PRINT*,"  NUMBER OF CRITICAL MODES = ",N
      PRINT*," "
      PRINT*,"  NUMBER OF ACTUATORS = ",NA
      PRINT*," "
      READ(5,*)(ALPHA(I),I=1,NA)
      READ(5,*)(BETA(I),I=1,NA)
      READ(5,*)(GAMMA(I),I=1,NA)
      READ(5,*)(NODE(I),I=1,NA)
      PRINT*," "
      PRINT*," "
      PRINT*,"                ORIENTATION OF ACTUATORS "
      PRINT*," "
      PRINT*,"    #          NODE      ALPHA       BETA      GAMMA "
      DO 1 I=1,NA
      PRINT*," "
    1 PRINT 300,I,NODE(I),ALPHA(I),BETA(I),GAMMA(I)
      READ(5,400)((PHI(I,J),I=1,354),J=1,N)
      READ(5,*)(ID(I),I=1,59)
      PI=3.14159265E0
      CON=PI/180.0
      NAA=NA+1
      DO 30 J=1,NA
      ALPHA(J)=ALPHA(J)*CON
      BETA(J)=BETA(J)*CON
      GAMMA(J)=GAMMA(J)*CON
      DO 10 K=1,59
   10 IF(ID(K).EQ.NODE(J))GO TO 20
   20 CONTINUE
      K=6*K-5
      DO 30 I=1,N
      B(I,J)=PHI(K,I)*COS(ALPHA(J))+PHI(K+1,I)*COS(BETA(J))
     1 +PHI(K+2,I)*COS(GAMMA(J))
   30 CONTINUE
      DO 999 KK=1,59
      ND=ID(KK)
      DO 999 IA=1,37
      IAA=5*IA-5
      A=IAA*CON
      DO 999 IB=1,37
      IBB=5*IB-5
      BE=IBB*CON
      IF(IAA+IBB.NE.90) GO TO 31
      G=90.0*CON
      GO TO 32
   31 CONTINUE
      COSA=COS(A)
      IF(COSA.LT.0.) COSA=-COSA
      IF(SIN(BE).LT.COSA) GO TO 999
```

```
      G=ACOS(SIN(BE)*COS(ASIN(COSA/SIN(BE))))
      G2=180*CON-G
   32 CONTINUE
      DO 998 IG=1,2
      IF(IG.EQ.1) GO TO 33
      IF(IAA+IBB.EQ.90) GO TO 998
      G=G2
   33 CONTINUE
      K=KK*6-5
      DO 6 I=1,N
      B(I,NAA)=PHI(K,I)*COS(A)+PHI(K+1,I)*COS(B)
     1 +PHI(K+2,I)*COS(G)
    6 CONTINUE
      DO 70 I=1,N
      BSQ(I)=0.0
      DO 70 K=1,NAA
      BSQ(I)=B(I,K)**2.0+BSQ(I)
   70 CONTINUE
      DO 90 I=1,N
      DO 90 J=1,N
      CB=0.0
      DO 80 K=1,NAA
   80 CB=B(I,K)*B(J,K)+CB
      ARG=CB/SQRT(BSQ(I))/SQRT(BSQ(J))
      IF(ARG.LE.1.0E00) GO TO 81
      ANGB(I,J)=0.0
      GO TO 82
   81 CONTINUE
      ANGB(I,J)=ACOS(CB/SQRT(BSQ(I))/SQRT(BSQ(J)))
   82 CONTINUE
      ANGB(I,J)=ANGB(I,J)/CON
      DO 101 I1=1,4
  101 IF(I.EQ.N1(I1)) GO TO 104
      DO 102 I2=1,3
  102 IF(I.EQ.N2(I2)) GO TO 105
      DO 103 I3=1,3
  103 IF(I.EQ.N3(I3)) GO TO 106
  104 DO 114 I1=1,4
  114 IF(J.EQ.N1(I1)) GO TO 110
      GO TO 111
  105 DO 115 I2=1,3
  115 IF(J.EQ.N2(I2)) GO TO 110
      GO TO 111
  106 DO 116 I3=1,3
  116 IF(J.EQ.N3(I3)) GO TO 110
      GO TO 111
  110 IF(ANGB(I,J).LT.82.0.OR.ANGB(I,J).GT.103.0) GO TO 90
      GO TO 998
  111 IF(ANGB(I,J).GT.76.0.AND.ANGB(I,J).LT.97.0) GO TO 90
      GO TO 998
   90 CONTINUE
      PRINT 200
      PRINT 500,A/CON,BE/CON,G/CON,ND
      PRINT 201
      PRINT 210,(I,I=1,N)
      DO 130 I=1,N
  130 PRINT 220,I,(ANGB(I,J),J=1,N)
```

```
200 FORMAT(1H1)
210 FORMAT(1X,5X,I7,11I10,/)
220 FORMAT(1X,/,I5,12F10.4,/,5X,12F10.4)
301 FORMAT(1X,30X,24HANGLES BETWEEN ROWS OF B)
300 FORMAT(1X,I5,I11,F11.2,2F10.2)
400 FORMAT(1P3E15.6)
500 FORMAT(1X,20X,6HALPHA=,F4.0,6H BETA=,F4.0,7H GAMMA=,F4.0,
   1 9H AT NODE:,I5,//)
998 CONTINUE
999 CONTINUE
    END
```

Vita

Robert Raymond Luter, Jr. was born on 24 March 1959 in Corpus Christi, Texas. He graduated from high school in Austin, Texas in 1977 and attended the University of Texas at Austin, from which he received the degree of Bachelor of Science in Aerospace Engineering in May 1981. Upon graduation, he received a commission in the United States Air Force through the ROTC program. He was then assigned to the School of Engineering, Air Force Institute of Technology, in June 1981.

UNCLASSIFIED

SECURITY CLASSIFICATION OF THIS PAGE

REPORT DOCUMENTATION PAGE

1a. REPORT SECURITY CLASSIFICATION Unclassified	1b. RESTRICTIVE MARKINGS
2a. SECURITY CLASSIFICATION AUTHORITY	3. DISTRIBUTION/AVAILABILITY OF REPORT Approved for public release; distribution unlimited.
2b. DECLASSIFICATION/DOWNGRADING SCHEDULE	
4. PERFORMING ORGANIZATION REPORT NUMBER(S) AFIT/GA/AA/82D-6	5. MONITORING ORGANIZATION REPORT NUMBER(S)
6a. NAME OF PERFORMING ORGANIZATION Air Force Institute of Technology 6b. OFFICE SYMBOL (If applicable) AFIT-EN	7a. NAME OF MONITORING ORGANIZATION
6c. ADDRESS (City, State and ZIP Code) Wright-Patterson AFB, Ohio 45433	7b. ADDRESS (City, State and ZIP Code)
8a. NAME OF FUNDING/SPONSORING ORGANIZATION 8b. OFFICE SYMBOL (If applicable)	9. PROCUREMENT INSTRUMENT IDENTIFICATION NUMBER
8c. ADDRESS (City, State and ZIP Code)	10. SOURCE OF FUNDING NOS. PROGRAM ELEMENT NO. / PROJECT NO. / TASK NO. / WORK UNIT NO.
11. TITLE (Include Security Classification) Optimal Sensor/Actuator Placement on a Large Space Structure	

12. PERSONAL AUTHOR(S)
ROBERT R. LUTER, JR., 1st Lt, USAF

13a. TYPE OF REPORT	13b. TIME COVERED	14. DATE OF REPORT (Yr., Mo., Day)	15. PAGE COUNT
MS Thesis	FROM ________ TO ________	84 March	81

16. SUPPLEMENTARY NOTATION

Approved for public release: IAW AFR 190-17.
LYNN E. WOLAVER
Dean for Research and Professional Development
Air Force Institute of Technology (ATC)
Wright-Patterson AFB OH 45433
8 Aug 84

17. COSATI CODES			18. SUBJECT TERMS (Continue on reverse if necessary and identify by block number)
FIELD	GROUP	SUB. GR.	Sensor/Actuator Placement; Large Space Structure; Observation Spillover; Control Spillover; Decentralized Controller

19. ABSTRACT (Continue on reverse if necessary and identify by block number)

The method of eliminating observation and control spillover is studied by making groups of reduced order controlled modes orthogonal to each other. These modes are the rows and columns of the system matrices which are calculated from the direction cosine matrix and the eigenvector matrix. The direction cosine matrix is determined from the locations and orientations of the sensors/actuators. The eigenvector matrix is determined from the NASTRAN finite element model of the large space structure. The decentralized controller can be made stable if the placement of the sensors/actuators cause the spill-over to be eliminated.

The program ANGLE is developed to calculate the angles between modes. After selecting a possible grouping of modes, problem angles are identified for improvement. These angles are then improved using the ORIENT program by manipulating the sensor/actuator placement model. Finally, the finite element model is changed to see its effect on the angles between the modes.

20. DISTRIBUTION/AVAILABILITY OF ABSTRACT UNCLASSIFIED/UNLIMITED ☒ SAME AS RPT. ☐ DTIC USERS ☐	21. ABSTRACT SECURITY CLASSIFICATION Unclassified
22a. NAME OF RESPONSIBLE INDIVIDUAL Maj Martin Wallace	22b. TELEPHONE NUMBER (Include Area Code) 513-255-2998 22c. OFFICE SYMBOL AFIT/ENY

DD FORM 1473, 83 APR

EDITION OF 1 JAN 73 IS OBSOLETE.

UNCLASSIFIED

SECURITY CLASSIFICATION OF THIS PAGE

END

FILMED

9-84

DTIC